Science of the Total Environment 818 (2022) 151827

Contents lists available at ScienceDirect

Science of the Total Environment

journal homepage: www.elsevier.com/locate/scitotenv

Potential contribution of distant sources to airborne *Betula* pollen levels in Northeastern Iberian Peninsula

Marta Alarcón [a,*], Cristina Periago [a], David Pino [a], Jordi Mazón [a], Maria del Carme Casas-Castillo [a], Jiang Ji Ho-Zhang [a], Concepción De Linares [b,c], Raül Rodríguez-Solà [a], Jordina Belmonte [c,d]

[a] Departament de Física, Universitat Politècnica de Catalunya (UPC), Barcelona, Spain
[b] Department of Botany, University of Granada, Granada, Spain
[c] Departament de Biologia Animal, Biologia Vegetal i Ecologia, Universitat Autònoma de Barcelona (UAB), Bellaterra, Spain
[d] Institut de Ciència i Tecnologia Ambientals (ICTA-UAB), Universitat Autònoma de Barcelona, Bellaterra, Spain

HIGHLIGHTS

- LRT over NE Spain is linked to the presence of an anticyclone over N Europe.
- Alberes pass and Ebro Valley are the main enter routes of *Betula* pollen to NE Spain.
- The Pyrenees, Galicia and Cantabria contribute 37% to the *Betula* LRT over Catalonia.
- French Central Massif and Black Forest/Vosges Massif contribute 63% over Catalonia.

GRAPHICAL ABSTRACT

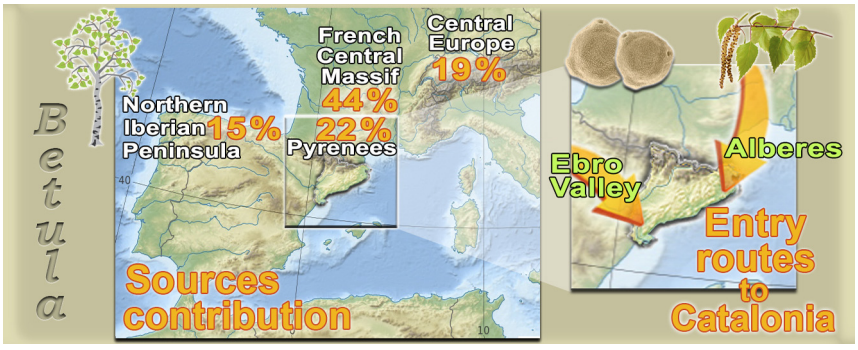

ARTICLE INFO

Article history:
Received 23 July 2021
Received in revised form 8 November 2021
Accepted 16 November 2021
Available online 20 November 2021

Editor: Pavlos Kassomenos

Keywords:
Pollen concentration peak and season
Source regions
Mesoscale and Lagrangian models
Orography
Role of long-range transport

ABSTRACT

Betula (birch) pollen is one of the most important causes of respiratory allergy in Northern and Central Europe. While birch trees are abundant in Central, Northern, and Eastern Europe, they are scarce in the Mediterranean territories, especially in the Iberian Peninsula (IP), where they grow only in the northern regions and as ornamental trees in urban areas. However, the airborne birch pollen patterns in Catalonia (Northeastern IP) show abrupt high concentrations in areas with usually low local influence. The intensity of the derived health problems can be increased by outbreaks due to long-range pollen transport. The present work evaluates the different potential contributions to Catalonia from the main source regions: Pyrenees, Cantabria, and the forests of France and Central Europe. To this end, we computed the Hybrid Single-Particle Lagrangian Integrated Trajectory (HYSPLIT) back trajectories of air masses associated with the main *Betula* pollen peaks occurring simultaneously over different Catalan monitoring stations, and we studied their provenance over a 15-year period. The Vielha aerobiological station on the northern slopes of the Central Pyrenees was used to identify the dates of the pollen season in the Pyrenean region. In order to better understand the role of the Pyrenees, which is the nearest of the four birch forested regions, we classified the pollen peaks in the other Catalan stations into three groups based on the relationship between the peak and the pollen season in the Pyrenees. Our analysis of back-trajectory residence time, combined with the associated pollen concentration, reveals that two principal routes other than the Pyrenean forest sustain the northerly fluxes that enter Catalonia and carry significant concentrations of *Betula* pollen. This study has also allowed quantifying the differentiated contributions of the potential source

* Corresponding author.
E-mail address: marta.alarcon@upc.edu (M. Alarcón).

http://dx.doi.org/10.1016/j.scitotenv.2021.151827

regions. In addition, the Weather Research Forecast (WRF) mesoscale model has been used to study three specific episodes. Both models, HYSPLIT and WRF, complement each other and have allowed for better understanding of the main mechanisms governing the entry of birch pollen to the region.

1. Introduction

The residence time of pollen grains and fungal spores in the atmosphere can be highly variable, but it is generally long enough (more than one day) for them to be transported away from sources of emission and settle thousands of kilometres away over land and/or oceans (Sofiev et al., 2006a). The size of pollen grains varies from 5 to 200 μm in diameter (Erdtman, 1992), making them about 5 to 50 times greater (in linear dimensions) than the particle size of conventional atmospheric aerosols. However, despite their much larger size, the grains of many pollen types (for example, anemophile pollen) behave similarly in their atmospheric dispersion to anthropogenic PM10 (particulate matter with a diameter of less than 10 μm). This similarity is due to the aerodynamic shape and low density of pollen, which drastically reduces its gravitational deposition and makes it more susceptible to atmospheric transport (Sofiev et al., 2006a, 2006b, 2006c). Long-range pollen transport is considered essentially episodic or sporadic, which means that an inverse mode treatment can be applied in order to define the probable regions of origin responsible for each episode. In other words, its trajectory is calculated backwards in time from the sampling site to the place of issue. In this line of work, several authors have used back trajectories and transport models to explain large-scale movements of pollen in Northeastern Iberian Peninsula (Belmonte et al., 2000, 2008; Fernández-Llamazares et al., 2012; Izquierdo et al., 2011, 2015a, 2015b; Sicard et al., 2019), Southern Iberian Peninsula (Hernández-Ceballos et al., 2011, 2015; García-Mozo et al., 2017), Northern and Central Europe (Sofiev et al., 2006a; Skjøth et al., 2007, 2009, 2015; Siljamo et al., 2008), and in Poland (Bogawski et al., 2019a). In other regions the distant transport has also been studied. In Beijing, China, Qin et al. (2019) determined the transport mechanisms and source regions for *Artemisia* pollen.

On the other hand, other studies have analysed the relationships between aerobiology and meteorological variables. Grinn-Gofroń et al. (2020) analysed the relation between airborne fungal spores load and climatic conditions in Turkey. Using the proxy of airborne fungal spores concentrations, Grinn-Gofroń et al. (2021) modelled the pathogen infection levels in the Turkish local trees. In addition to the well-known allergic respiratory diseases that some types of pollen cause, recent studies show that pollen exposure weakens the immunity against certain seasonal respiratory viruses. Damialis et al. (2021), in a preliminary study, analysed the relationship between SARS-CoV-2 infection, airborne pollen, and meteorological variables in 31 countries across the globe, finding that airborne pollen, in synergy with humidity and temperature, explained, on average, 44% of the infection rate variability.

Birch trees are abundant in Central, Northern and Eastern Europe, but they are scarce in the Mediterranean territories (De Bolòs et al., 1990), where the northern regions constitute the southern border of the distribution area. In the Iberian Peninsula (IP), they grow only in the Pyrenean, Galician and Cantabrian regions under certain environmental conditions of altitude and as ornamental trees in urban areas. Birch (*Betula*) pollen is transported by wind and affects human health by causing seasonal hay fever, pollen-related asthma, and other allergic diseases (Heinzerling et al., 2009; Spieksma et al., 1995; D'Amato et al., 2007; Emberlin et al., 1993, 1997; Myszkowska and Majewska, 2014; Myszkowska and Piotrowicz, 2009). Regional and long-range transport (LRT) of *Betula* pollen in Europe have been described in several studies (Skjøth et al., 2007; Siljamo et al., 2008; Sofiev et al., 2015; Grewling et al., 2016), as well as the changes that LRT can introduce in its dynamics by enlarging and modifying the pollen season (Bogawski et al., 2019b). A recent study obtains a positive and statistically significant trend in the frequency of atmospheric circulation types favourable for high concentrations of *Betula* pollen in Poland (Ojrzyńska et al., 2020).

Betula pollen is a common cause of pollinosis in Northwestern Spain, where between 13% and 60% of people who are immunosensitive to pollen grains respond positively to their allergens (Aira et al., 2001; Dopazo, 2001). A recent study (Pfaar et al., 2017) on clinical thresholds and periods of pollen exposure times has determined the threshold 100 pollen/m^3 for birch as a high value for pollen-induced rhinoconjunctivitis. In Catalonia (NE of Spain) birch is scarce, but under certain meteorological conditions that favour LRT, the intensity of the pollen derived health problems may increase (Izquierdo et al., 2017; Pereira et al., 2006). Although far from this high threshold value, these outbreaks introduce considerable amounts of highly allergenic pollen during the birch pollen season in Central/Northern Europe and the Pyrenees. It is known that the thresholds of allergenicity vary between localities depending on the usual pollen concentrations, presenting lower thresholds those localities with lower concentrations (De Weger et al., 2013).

Models are good tools for studying and understanding the atmospheric mechanisms that cause pollen outbreaks at sites with little or no presence of it (Mahura et al., 2007; Robichaud and Comtois, 2017; Negral et al., 2021). Previous works have established France and Central Europe as potential source areas of the *Fagus* (Belmonte et al., 2008) and *Ambrosia* (Belmonte et al., 2000; Fernández-Llamazares et al., 2012, 2014) pollen grains that arrive in the NE Iberian Peninsula. Moreover, the effect of the orographic barrier of the Pyrenees has also been evaluated in regard to the LRT of *Betula* pollen (Izquierdo et al., 2017). However, up to present, the potential contribution of the different source regions has not been evaluated. In the present work we have focused on establishing the differentiated contribution of the probable source regions responsible for LRT over Catalonia. In order to establish this potential contribution while also bearing in mind that LRT would be indicated by simultaneous peaks, we study here the provenance of the air masses leading to the main simultaneous *Betula* pollen peaks that are detected in the Catalan monitoring stations. In addition, the Vielha Pyrenees Station pollen database has provided information about the birch pollen season in the Pyrenean region.

Large scale models such as the Hybrid Single-Particle Lagrangian Integrated Trajectory (HYSPLIT) are useful for computing a large number of trajectories in order to obtain the mean flow of the air masses. However, they lose representativeness when individual trajectories are analysed. In complex orography, such as the NE of the Iberian Peninsula, the use of a mesoscale model improves the accuracy and reliability of the trajectories (Belmonte et al., 2008; Hernández-Ceballos et al., 2014; Izquierdo et al., 2017). One of the most widely used mesoscale models in air quality modelling and atmospheric transport is the Weather Research Forecast (WRF). The WRF model has been applied to different research topics in a wide range of spatial scales, including the global scale, the mesoscale, and the microscale (Skamarock et al., 2008). In our study, we have taken advantage of the complementary information provided by the simultaneous use of a mesoscale model and a lagrangian model to analyse particular episodes.

This paper has focused in the atmospheric transport of *Betula* pollen over a 15-year period in order to assess its contributions from long-distant sources to the pollen records obtained at six aerobiological stations in Catalonia. To discriminate between the LRT of *Betula* pollen and the influence of local pollen, we hypothesized that LRT would be identified by simultaneous peaks at most of the Catalan monitoring stations. Subsequently, we used back trajectories to describe the synoptic flux responsible for transport on peak days of simultaneous pollen arrivals. Four potential source regions with a high presence of birch trees have been defined, based on their proximity to the Catalan aerobiological stations. Since the closest region is the

Pyrenees massif, to better identify the contribution of this massif we classified the peaks into three groups based on the relationship between the dates of these peaks and the peak pollination dates in the Pyrenees. The study evaluates the differentiated contributions of four regions to the *Betula* pollen levels registered in Catalonia, specifically by: i) isolating the peaks (based on the 95th percentile) that are produced simultaneously in at least four of the six aerobiological stations covering the Catalan territory; ii) computing the HYSPLIT back trajectories for the peak dates in order to characterize the associated flow directions and source regions; iii) classifying the peaks into three clusters: previous, coincident, and later to pollination in the Pyrenees; iv) using HYSPLIT and the WRF mesoscale model to analyse three case studies, one from each cluster; and v) quantifying the potential contribution of long-range pollen transport according to the levels measured in Catalonia.

2. Material and methods

2.1. Area of study

Catalonia is located in the northeast of the Iberian Pennsula, bordering France and the Pyrenees to the north and the Mediterranean Sea to the east (Fig. 1). Complex terrain can be found along the coast due to littoral and pre-coastal mountain ranges and in the north due to the Pyrenees and pre-Pyrenees mountain ranges. The forests are located in the mountainous areas and are composed mainly of Mediterranean species (*Quercus ilex* and *Pinus halepensis*); while the Pyrenees and pre-Pyrenees above 1500 m comprise Eurosiberian forests with conifers (*P. sylvestris* and *P. mugo* subsp. *uncinata*) and deciduous forests with *Quercus* and *Betula* trees. Our study focuses on birch pollen (*Betula*) because it is not common in the Mediterranean area, which ensures that large quantities registered on certain days can be attributed to LRT. Northern, Central, and Eastern Europe are abundant with four different species of birch: *B. humilis*, *B. nana*, *B. pendula*, and *B. pubescens*. The last two species can be found in Catalonia between 800 and 2200 m a.s.l. (De Bolòs et al., 1990), mainly on the northern face of the Pyrenees, but rarely in the Mediterranean regions. Fig. 3 shows the high resolution distribution map of the relative probability of presence for the *Betula* genus in Western Europe based on Beck et al. (2016).

2.2. Pollen record

This study analyses daily *Betula* pollen concentrations recorded during the birch flowering season (from 1st March to 31st May) for the 15-year period from 2005 to 2019. This dataset was obtained from six pollen-monitoring sites located in NE Spain (Fig. 1): Barcelona (BCN; 41°24′N, 2°09′E, 93 m a.s.l.), Bellaterra (BTU; 41°30′N, 2°06′E, 245 m a.s.l.), Girona (GIC; 41°59′N, 2°50′E, 98 m a.s.l.), Lleida (LLE; 41°37′N, 0°38′E, 202 m a.s.l.), Manresa (MAN; 41°44′N, 1°30′E, 291 m a.s.l.), and Tarragona (TAU; 41°07′N, 1°15′E, 44 m a.s.l.). Samples were obtained daily from Hirst samplers (Hirst, 1952) following the standardized method proposed by the European Aerobiological Association (Galán et al., 2014), and they were analysed following the standardized Spanish method (Galán et al., 2007). Following these methods, and in order to determine the pollination period of birch forests in the Pyrenees, we used daily pollen concentrations recorded at the Vielha aerobiological station (VIE; 42°42′N 0°47′E, 980 m.a.s.l.), located on the northern slope of the Central Pyrenees.

A threshold value identifies the *Betula* pollen peaks: daily pollen concentrations higher than each year's 95th percentile. We estimated local flowering in the Pyrenees region for each year from the date of the main pollen annual peak in VIE. Therefore, the pollen simultaneous peaks in the other stations were categorised into three clusters according to their date of occurrence: (1) previous to the peak pollination date in Vielha station (hereinafter referred to as PREVIOUS); (2) coincident with the Vielha peak pollination date (hereinafter referred to as COINCIDENT); and (3) later than the peak pollination date in Vielha (hereinafter referred to as LATER).

The summary of the airborne *Betula* pollen dynamics in the study period (March–May 2005–2019) is shown in Fig. 2.

2.3. HYSPLIT back-trajectories and source regions

We computed two back trajectories (00 and 12 UTC) of 96-h lengths at 1500 m a.s.l. using a time-step of 1 h, ending in the aerobiological stations, for each day of the identified simultaneous peaks. We chose this height because approximately corresponds to the 850 hPa standard pressure level that is the approximate boundary between the surface wind regime and the free troposphere (Artz et al., 1985). It can be taken as representative of the mean atmospheric transport at a synoptic scale within the lower and upper boundary layers. Moreover, a relationship between the 850 hPa wind direction and the prevailing weather patterns associated with the passage of cyclonic waves is well established (Dayan and Lamb, 2003). On the other hand, several tentative exercises using modelling and observed vertical distribution of pollen from lidar observations in the region of Barcelona conducted by Sicard et al. (2016a, 2016b, 2017, 2019, 2021) concluded that the vertical structure of the airborne pollen is mainly controlled by the vertical mixing within the boundary layer.

The trajectories were calculated by using computed vertical velocity with the Hybrid Single-Particle Lagrangian Integrated Trajectory Model (HYSPLIT) of the Air Resources Laboratory (ARL; http://www.arl.noaa.gov/ready/HYSPLIT4.html; Draxler and Rolph, 2003). We used meteorological data from the Global Data Assimilation System (GDAS) of the U.S. National Climate Data Center (NCAR), with 1° latitude/longitude horizontal resolution. The meteorological data used by HYSPLIT is bi-linearly

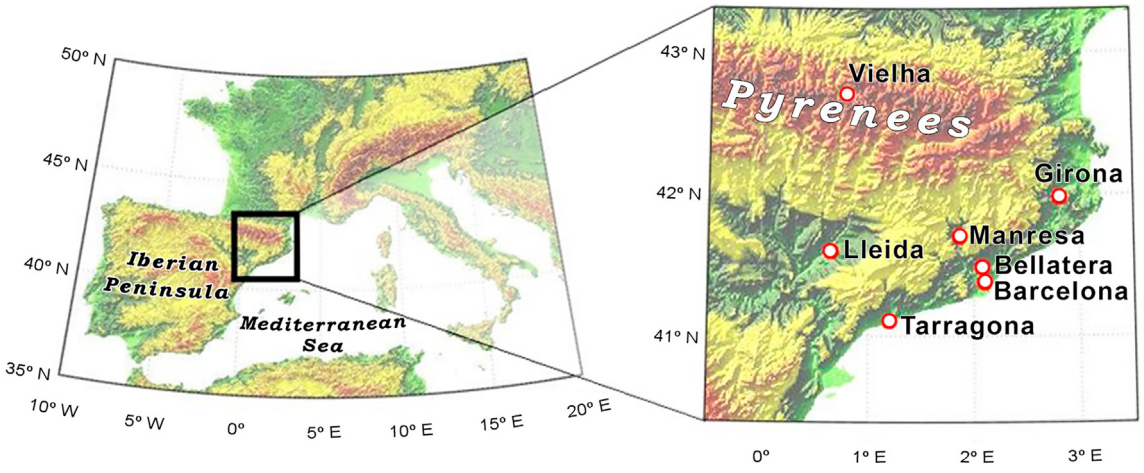

Fig. 1. Location of the Catalan sampling sites.

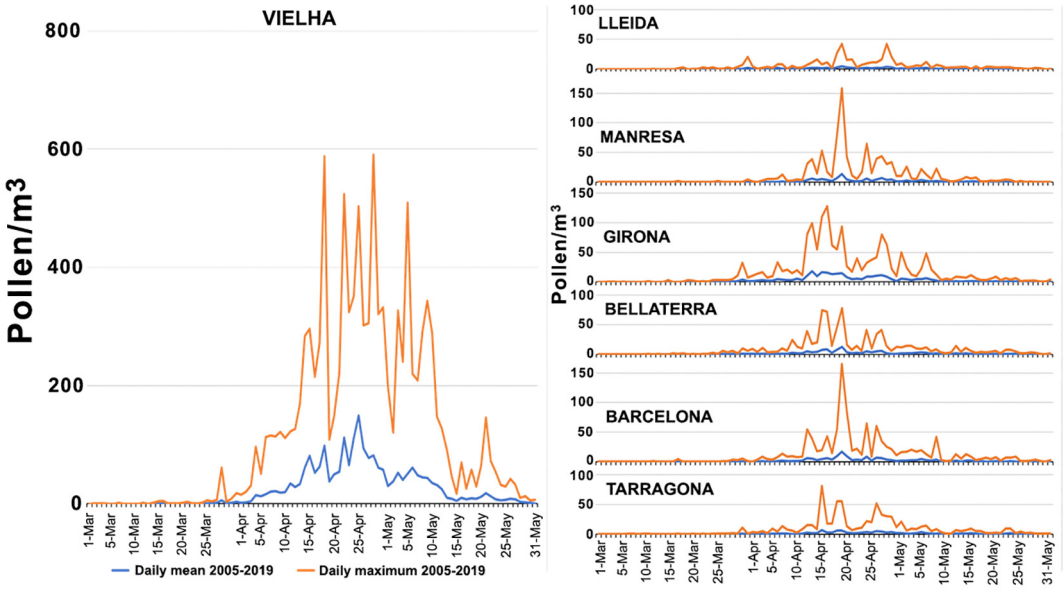

Fig. 2. Daily mean concentration and daily maximum (Pollen/m^3) during the study period for Vielha and the other 6 stations.

interpolated in space and linearly interpolated in time to the location and time of the subsequent time step. If important variations in the meteorological fields occur between grid points or between meteorological data output times, errors in the trajectory segments may result. Several studies (Wotawa and Kröger, 1999; Begum et al., 2005) have tried to validate various trajectory analysis methods, mostly through direct comparison with known sources. Upper bounds for average absolute horizontal and vertical errors after 120 h travel time were 400 km and 1300 m, respectively (Stohl, 1996). Due to turbulent mixing, there is a loss of reliability in the trajectories computed in the boundary layer.

To better understand the transport mechanisms, we analysed one episode from each cluster using both the HYSPLIT large scale model (greater than 100 km resolution) and the WRF mesoscale model. HYSPLIT back-trajectories were computed at 1500 m a.s.l. by leaving a new back trajectory (48-hour length) every 3 h, from 18 UTC of the peak day and over the previous 24 h. The synoptic charts corresponding to the dates of these

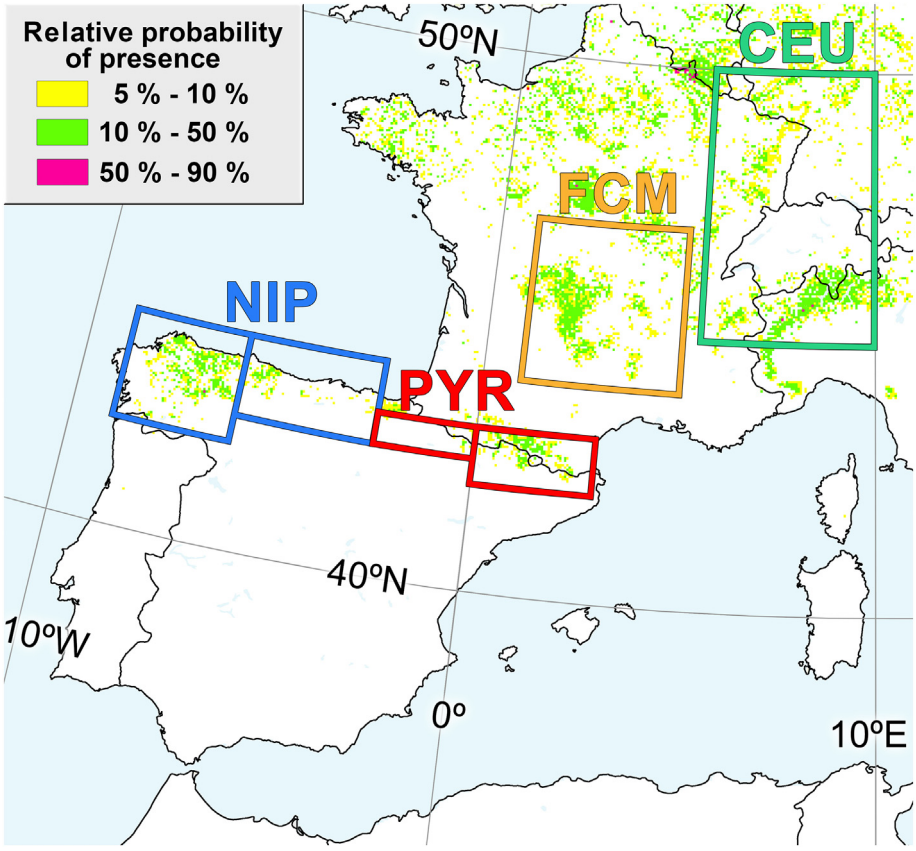

Fig. 3. High resolution distribution map estimating the relative probability of presence for the genus *Betula* after Beck et al. (2016). The rectangles correspond to the four source regions considered here: Central Europe (CEU), French Central Massif (FCM), Northern Iberian Peninsula (NIP), and Pyrenees (PYR).

three episodes were also obtained from the ARL (https://www.ready.noaa.gov/READYamet.php). The WRF model and the set up used are described in Section 2.4.

Based on the map in Fig. 3, we considered four different regions with a high abundance of birch trees as probable sources of the pollen collected at the Catalan stations: Pyrenees (PYR), Northern Iberian Peninsula (NIP, which includes the Cantabrian Mountains and the Galicia region), French Central Massif (FCM), and Central Europe (CEU, mainly Black Forest and Vosges Massif). Table SM1 (Supplementary Material) specifies the coordinates defining the boxes considered as the source regions. For each of the four regions, we computed the total number of 1-hour time steps. The average residence time of the back trajectories in each region was obtained by dividing the number of 1-hour time steps into the number of back trajectories in the region. Based on the average residence time in each source region, we arrived at a first estimate of each region's contribution to the *Betula* Pollen Integral of the study period, collected in Catalonia.

2.4. WRF mesoscale model

We use the WRF model v4.0 (http://www.wrf-model.org/index.php) to study the three specific episodes, one from each cluster, mentioned above. The WRF model is viable as a next-generation mesoscale model for both research and operational forecasting, and it was designed in a joint effort by NCAR, NOAA, NCEP, the Earth System Research Laboratory (ESRL), the Center for Analysis and Prediction of Storms (CAPS) at the University of Oklahoma, and the Federal Aviation Administration (FAA). WRF is a compressible non-hydrostatic finite difference model that runs the conservation equations (mass, momentum, energy) describing the atmosphere. The WRF model is used to obtain the evolution of pressure, temperature, wind field, and surface fluxes on the days of the events, and it subsequently calculates the back-trajectories (Skamarock et al., 2008). We define two nested domains at horizontal resolutions of 27 km and 9 km (Fig. 4). The smallest domain is centred over the general area of individual extreme events, covering a total of 417 × 291 km^2. In the vertical, 45 η-vertical levels are defined. We use the MRF scheme for parameterizing the planetary boundary layer (Hong and Pan, 1996), the RRTM scheme for modelling longwave radiation (Mlawer et al., 1997), the MM5 shortwave scheme for modelling shortwave radiation (Dudhia, 1989), the WSM 3-class scheme for microphysics parameterization (Hong et al., 2004), and the Noah land surface model (Chen and Dudhia, 2001). No cloud parameterization is used for the smallest domain, as its horizontal resolution is 9 km. Initial and boundary conditions were updated every 6 h with information obtained from the operational ECMWF model. WRF back-trajectories have been drawn using the software https://www2.mmm.ucar.edu/wrf/users/docs/ripug.htm, available at https://www2.mmm.ucar.edu/wrf/users/download/get_sources_pproc_util.html.

3. Results

3.1. General overview

A total of 43 simultaneous peaks (concentration > 95th percentile in at least four of the six stations) were obtained over the 15-year period: 13 of them were PREVIOUS to the pollen season in Vielha station; 17 were LATER; and 13 were COINCIDENT. Table 1 shows the dates and concentrations (Pollen/m^3) registered at the six stations. Because the criterion was simultaneity in at least four of the six stations, the asterisk indicates those values lower than the 95th percentile (blanks indicate no data). BCN was the station where these episodes had the greatest presence (96%, not shown), while LLE had the least presence (68%). The episodes were highly variable in time. The PREVIOUS ones are produced mainly during the second and third weeks of April, the COINCIDENT during the fourth week of April, and the LATER during the last week of April and the first three weeks of May.

The pollen concentration collected during the peak dates (or episodes as we name them in this paper) differed greatly between them, even within the same cluster, and they also differed between stations. For example, in the PREVIOUS peak produced on 19th of April 2007, the pollen

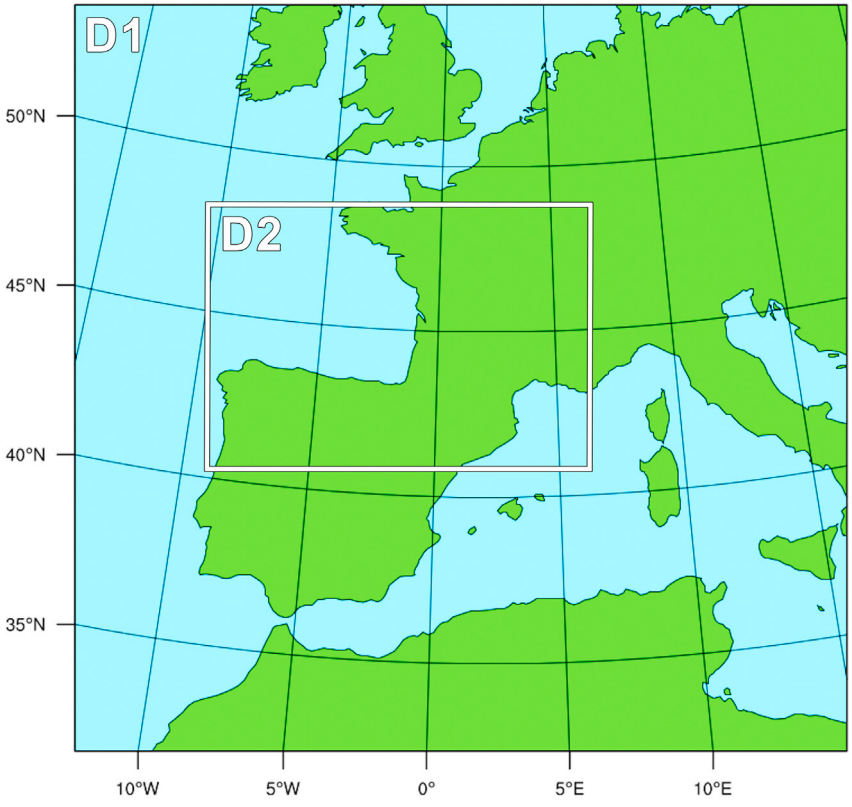

Fig. 4. Nested domains defined in the WRF numerical simulations: D1 (horizontal resolution 27 × 27 km^2) and D2 (horizontal resolution 9 × 9 km^2).

Table 1
Dates and concentrations (Pollen/m^3) of the peak days for the three clusters. In bold the three cases analysed in Section 3.4. Asterisk: values lower than the 95th percentile (blanks indicate no data).

	BCN	BTU	LLE	GIC	MAN	TAU
Previous						
13/04/2005	39	18	11	99	15	27
22/04/2005	22	10	0*	24	10	0*
15/04/2007	20	74	0*	110	81	53
18/04/2007	**43**	**17**	**4**	**39**	**1***	**80**
19/04/2007	165	78	8	93	1*	158
12/04/2014	55	39	4	81	5*	32
14/04/2015	1	2	4	6	4	4
01/05/2016	16	12	10	50	21	11
02/05/2016	12	14	3	21	3	4
07/04/2017	10	1	8	15	14	13
16/04/2018	43	72	1	128	12	8
18/04/2018	55	45	27	44	55	18
19/04/2018	48	57	43	18	55	18
Coincident						
25/04/2008	8	10	0*	37	4	2
26/04/2008	12	21	0*	34	11	7
27/04/2008	8	5	0*	11*	6	4
24/04/2009	65	41	7	32	13	64
26/04/2010	14	5*	5*	41	11	13
27/04/2010	**34**	**15**	**17**	**81**	**18**	**40**
28/04/2010	25	14	42	64	30	30
29/04/2010	21	6	15	22	11	25
09/04/2011	10	25	4	15	0*	1*
24/04/2013	26	4*	10	20*	22	9
16/04/2014	13	15*	6	48*	18	17
21/04/2015	19	8	1	17	7	5
14/04/2017	11	8	16	11	2	1
Later						
26/04/2006	61	34	20	20	53	40
27/04/2006	23	41	7	20	33	44
02/05/2009	18	9	3	24	6*	27
05/05/2009	19	9	1*	6*	13	22
27/04/2011	6*	4	3	1*	4	6
12/05/2012	13	15	1*	9	5	0*
13/05/2012	6	4	4		5	4
14/05/2012	11	2*	4	2*	5	7
06/05/2013	11	12	10	48	9*	
18/04/2014	**11**	**22**	**8**	**55**	**25**	**3***
23/04/2015	9	5	0	11	1	1
28/04/2015	7	4	1	1	4	0
14/05/2016	13	11	1	7	6	8
19/04/2017	8	15	13	7	13	17
20/04/2017	9	10	6	1	11	8
05/05/2019	4	6	1	4	11	5
12/05/2019	6	7	3	1	7	2

concentration was high in BCN and TAU, but low in LLE and MAN. The PREVIOUS episode registered on 14th of April 2015 was simultaneous at the 6 stations, indicating the existence of LRT, but the pollen concentrations registered in all stations was very low. The same sort of inhomogeneity in the pollen concentrations was found in the COINCIDENT and LATER clusters, but at generally lower values.

The sum of the *Betula* pollen concentrations (Table 2) during the peak days, considering the six stations and the three clusters, was 4880 Pollen*day/m^3, representing 38% of the *Betula* Pollen Integral (PPin) over the 15-year period. During the PREVIOUS (2510 Pollen*day/m^3) peaks it was twice more than in COINCIDENT (1258 Pollen*day/m^3) and LATER (1112 Pollen*day/m^3) peaks. Moreover, the average amount contributed by each peak was greater in PREVIOUS (32 Pollen/m^3) than in COINCIDENT (21 Pollen/m^3), and it was almost triple that in LATER (11 Pollen/m^3).

Although, globally, the PREVIOUS cluster presented the largest pollen concentrations and the LATER the smallest, the records differed considerably between sites (Table 2), with GIC being the station registering the highest sum of peak concentrations (1290 Pollen*day/m^3), followed by

Table 2
Betula Pollen Integral (PPin) of the period (from March to May 2005–2019) (Pollen*day/m^3); sum of the pollen concentrations on peak days for each cluster (Pollen*day/m^3); percentage of this sum with respect to the *Betula* Pollen Integral in the period; average concentration by peak in each cluster (Pollen/m^3); and sum of percentages. Last column: pollen sum of the six stations.

	BCN	BTU	LLE	GIC	MAN	TAU	ALL
Pollen Integral (PPIn) March–May 2005–2019	2420	1994	998	4274	1542	1705	12,933
Previous							
Sum (peak days)	529	439	121	729	270	423	2510
Percentage	22%	22%	12%	17%	18%	25%	19%
Average by peak	41	34	9	56	21	33	32
Coincident							
Sum (peak days)	265	152	118	353	152	218	1258
Percentage	11%	8%	12%	8%	10%	13%	10%
Average by peak	27	15	12	35	15	22	21
Later							
Sum (peak days)	227	208	83	209	195	192	1112
Percentage	9%	10%	8%	5%	13%	11%	9%
Average by peak	13	12	5	12	11	11	11
Sum of concentrations and percentages	1021 42%	799 40%	322 32%	1291 30%	617 41%	833 49%	4880 38%

BCN (1021 Pollen*day/m^3). The LLE station registered the lowest values (322 Pollen*day/m^3); while BTU (799 Pollen*day/m^3), MAN (617 Pollen*day/m^3), and TAU (832 Pollen*day/m^3) had similar values, that were nearly half that of GIC. The pollen concentration registered at the different sites followed the above-mentioned pattern in which the PREVIOUS peaks were the highest in all stations while also having the highest average concentrations of pollen by peak. Comparatively, LLE and MAN show lower pollen concentration in the PREVIOUS episodes than the other stations. Differences in total pollen concentration were also evident across stations. As mentioned in the previous paragraph, the contribution of the episodes to the *Betula* PPIn collected in all stations accounted for 38%, but they represented nearly 50% at TAU while they were only 30% at GIC.

3.2. Residence time

A total of 516 HYSPLIT back trajectories (49,536 time-steps) corresponding to the 43 simultaneous peaks were computed. Back-trajectories ending at the six aerobiological stations are shown in the Fig. SM1 (Supplementary material), grouped into the three clusters. Most of the trajectories corresponded to northern, northeastern, and northwestern fluxes. The lengths of the trajectories were quite similar for the three clusters, travelling an average distance of about 2800 km during the 96 h. The PREVIOUS cluster had slightly faster trajectories (31 km/h) than the other two (30 km/h, COINCIDENT; 27 km/h, LATER). For the PREVIOUS episodes, the back trajectories represented a northerly flux from mostly France and Central Europe, crossing the PYR source region from north to south and taking a short route over this region. Conversely, back trajectories had long paths over PYR and NIP in the COINCIDENT episodes while being able to load high pollen concentrations from these regions. In contrast, very few back trajectories came from NIP in the LATER episodes, which prevailed in the FCM and CEU air-masses and entered Catalonia crossing PYR in curved trajectories, also in long paths over this region.

Table 3 shows the average residence time of the back trajectories in each of the four probable source regions for the six aerobiological stations, computed separately for the three clusters. Considering all the stations and episodes, the estimated percentage of residence time for the back trajectories was 26% in PYR, 18% in NIP, 40% in FCM, and 16% in CEU. However, similarly to what was found in the analysis of concentrations, remarkable differences exist between stations, suggesting different transport patterns. In the PREVIOUS episodes, the station that was most influenced by all four regions, highlighting FCM, was GIC. For the LATER episodes in GIC, FCM was also the most relevant, while PYR was the least. However, the PYR region was remarkable in the LATER cluster for other sites such as LLE and MAN. In contrast, the NIP region was residual in all stations for

Table 3
Average residence time (in hours) of the HYSPLIT back trajectories in the four source regions for the six aerobiological stations, and the three clusters of episodes.

	PYR	NIP	FCM	CEU
Previous				
BCN	0.73	0.58	3.85	1.15
BTU	0.77	0.69	3.69	0.88
GIC	1.31	1.35	5.46	3.15
LLE	1.19	0.46	2.27	2.31
MAN	0.90	0.58	2.46	0.92
TAU	0.96	0.62	3.54	1.00
Average	0.97	0.71	3.55	1.57
Percentage	14%	11%	52%	23%
Coincident				
BCN	3.15	2.65	2.96	1.85
BTU	3.08	3.04	2.88	1.54
GIC	2.85	2.04	3.88	2.69
LLE	2.81	6.19	2.04	0.15
MAN	5.19	4.00	3.35	0.69
TAU	1.35	4.35	2.81	1.04
Average	3.10	3.70	3.00	1.30
Percentage	28%	33%	27%	12%
Later				
BCN	2.44	0.24	3.59	1.76
BTU	2.68	0.50	3.65	1.71
GIC	1.94	0.24	6.56	2.29
LLE	3.41	0	3.53	0.59
MAN	3.38	0.38	3.53	1.03
TAU	2.50	0.56	2.85	1.29
Average	2.70	0.30	4.00	1.40
Percentage	32%	4%	47%	17%
SUM averages	6.80	4.70	10.5	4.30
Total percentage	26%	18%	40%	16%

the LATER episodes, representing only 3.8% of the total time-steps. Regarding the COINCIDENT episodes, the PYR provenance had relevance in MAN. However, for this cluster, the NIP provenance was also prominent in LLE and TAU. In contrast, the residence time in the CEU region for LLE was near null for this cluster.

Table 4 shows the residence time of the back trajectories in the different source regions for all three clusters and is expressed in percentages for each station. FCM was the most influential source region at all the sites except for MAN, where PYR was slightly higher. The residence time in PYR was high in general, but especially in MAN and LLE. GIC was the site most influenced by the CEU fluxes while MAN was the least. The provenance distribution of the LLE site was similar to MAN, but with a higher percentage of fluxes coming from the NIP region. In fact, regarding the percentages related to the NIP provenance, LLE registered the highest.

Fig. 5 shows the residence time of the back trajectories in each source region (in hours) averaged for the six stations. From this figure and the percentages shown in Table 3, it follows that PREVIOUS episodes corresponded to fast air masses coming mainly from Europe (FCM represented 52% and CEU 23%). The COINCIDENT episodes had the longest residence time in the source regions, with NIP, PYR, and FCM standing out at, respectively, 33%, 28%, and 27%. The LATER episodes were predominated by FCM transport (47%) and PYR transport (32%), while NIP transport was residual (4%). This fact reveals that the LATER episodes contained an important mix of pollen coming from Europe and the Pyrenees. On the other

Table 4
Percentage of residence time of the back trajectories in each source region for the six aerobiological stations.

	PYR (%)	NIP (%)	FCM (%)	CEU (%)
BCN	25	14	42	19
BTU	26	17	41	16
GIC	18	11	47	24
LLE	30	27	31	12
MAN	36	19	35	10
TAU	21	24	40	15

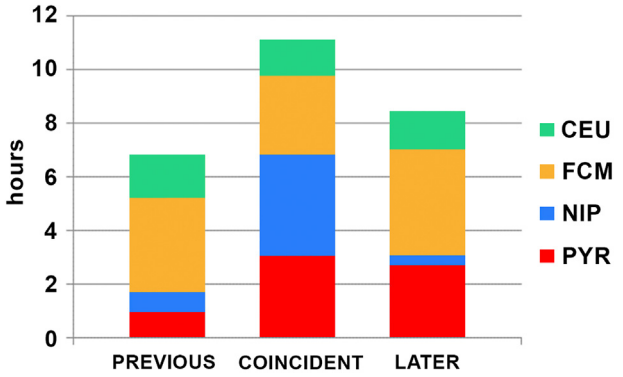

Fig. 5. Residence time of the back trajectories in each source region, expressed in hours, for the three clusters of episodes.

hand, it is remarkable that the residence time in the CEU source region was similar in the three clusters, with non-negligible percentages (around 17%), in spite of the long distance.

3.3. Estimated contributions from the source-regions

Based on the residence time in each region that is shown in Table 3, we have quantified the contribution of the four source regions to the LRT over Catalonia. The pollen concentrations obtained for the three clusters of episodes are shown in Table 5. Almost half of the pollen came from FCM (44%). PYR was the second most important source, contributing 22% of the pollen collected during the episodes. The most distant source region, CEU, contributed 19%, and NIP provided the least amount (15%). Regarding the impact on the clusters, the source regions that contributed the most were FCM for PREVIOUS (1309 Pollen*day/m^3) and LATER (521 Pollen*day/m^3), and NIP for COINCIDENT (421 Pollen*day/m^3). Also notable is the CEU contribution to the PREVIOUS episodes (579 Pollen*day/m^3).

3.4. Three case studies

To better understand the influence of the mesoscale, we have selected cases that show high variability in the concentrations between stations (Table 1, in bold). The PREVIOUS episode occurred on the 18th of April 2007 registered the highest values in the cluster during the two consecutive days 18 and 19, but with very low concentrations in LLE and MAN. Similarly, the other two case studies, the 27th of April 2010 (COINCIDENT cluster) and the 18th of April 2014 (LATER cluster), corresponded to dates with low concentrations in some of the stations. In order to avoid an excess of figures, only the back trajectories of BCN, TAU, LLE, and MAN are shown. GIC is less interesting from the point of view of LRT, since it is the closest to the Pyrenees and has the greatest presence of local birch. The figures

Table 5
Estimates of the pollen concentration provided by each source region based on the residence time of the back trajectories.

	PYR	NIP	FCM	CEU
Previous				
Residence time (%)	14.3	10.5	52.1	23.1
Concentration (Pollen*day/m3)	359	263	1309	579
Coincident				
Residence time (%)	27.7	33.4	26.9	12.0
Concentration (Pollen*day/m3)	348	421	339	150
Later				
Residence time (%)	32.3	3.8	46.8	17.1
Concentration (Pollen*day/m3)	359	42	521	190
SUM (Pollen*day/m^3)	1067	726	2168	920
Pollen from the regions (in %)	22	15	44	19

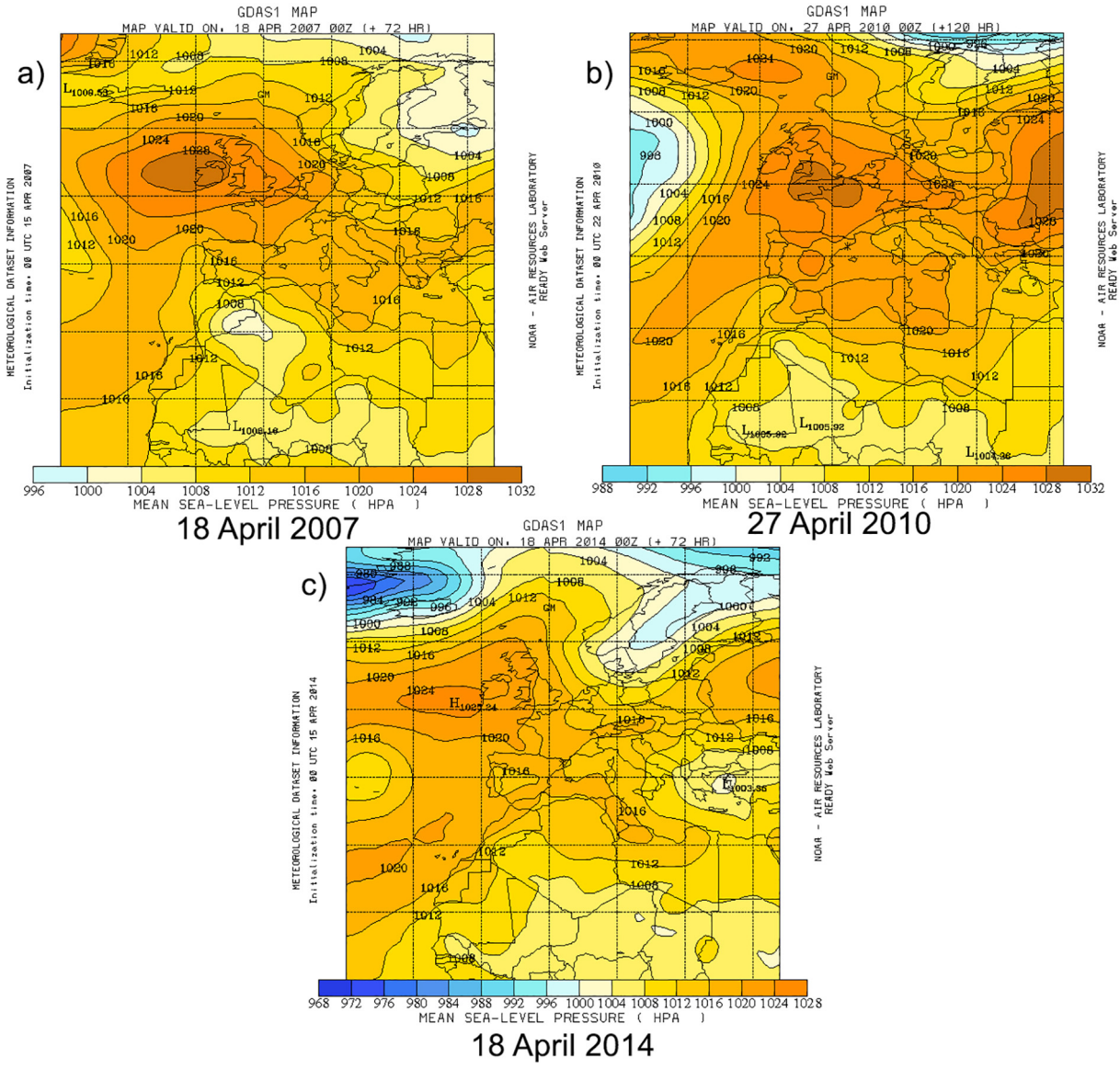

Fig. 6. Mean sea level pressure (hPa) for a) the PREVIOUS episode of 18 April 2007, b) the COINCIDENT episode of 27 April 2010, and c) the LATER episode of 18 April 2014.

corresponding to GIC and BTU are available in the Supplementary Material (Figs. SM2 to SM7).

Fig. 6 shows the surface synoptic situations for the three cases, in which can be observed the presence of high-pressure systems over Northwestern Europe.

3.4.1. PREVIOUS episode on the 18th of April 2007

The peak detected on 18th of April 2007 lasted until the 19th of April, and it occurred simultaneously at five of the six stations (MAN being the exception), with the highest values occurring at BCN and TAU, and the lowest at LLE. The values for the following day (19th of April) in BCN and TAU were the highest in the entire record. Fig. 6a shows the synoptic chart (mean sea level pressure) at 00 UTC, where we can see a high pressure system west of the British Islands that favours displacement of the air masses from Central Europe to the northeastern part of the IP, with this flux being reinforced by the low-pressure system situated over East Scandinavia. According to the integrated back trajectories computed by HYSPLIT for this episode (Fig. 7), the air mass penetrates into Catalonia through the Alberes passage, coming from CEU (Massif of the Vosges and the Black Forest) and also from FCM (French Central Massif). The figure shows the trajectory frequency (number of trajectories passing through each 1°x1° grid square, divided by the number of trajectories and expressed in percentage). It is clear that the back trajectories reach BCN and TAU from the northwest, while this flow did not influence LLE and TAU that registered low pollen values under the influence of Mediterranean air masses.

The back trajectories computed from the WRF model (Fig. 8) have similar paths for BCN (blue), TAU (green), and LLE (red) in D1 (27 km resolution, Fig. 8a). They concur with HYSPLIT in that they come from CEU, and enter Catalonia through the Alberes passage, although from a more western region in the case of LLE. The one for MAN (purple) followed a Mediterranean path similarly to that obtained from HYSPLIT. The results for D2 (9 km resolution, Fig. 8b) show a northerly flux and entrance through the Alberes passage for all six stations. However, in addition to LLE for this domain, the TAU and MAN stations also had a more westerly provenance (Western France).

3.4.2. COINCIDENT episode on the 27th of April 2010

The episode registered on the 27th of April 2010 presents a synoptic situation in which the high-pressure system is slightly displaced to the southeast, centred over Southern England (Fig. 6b). What is more, a secondary

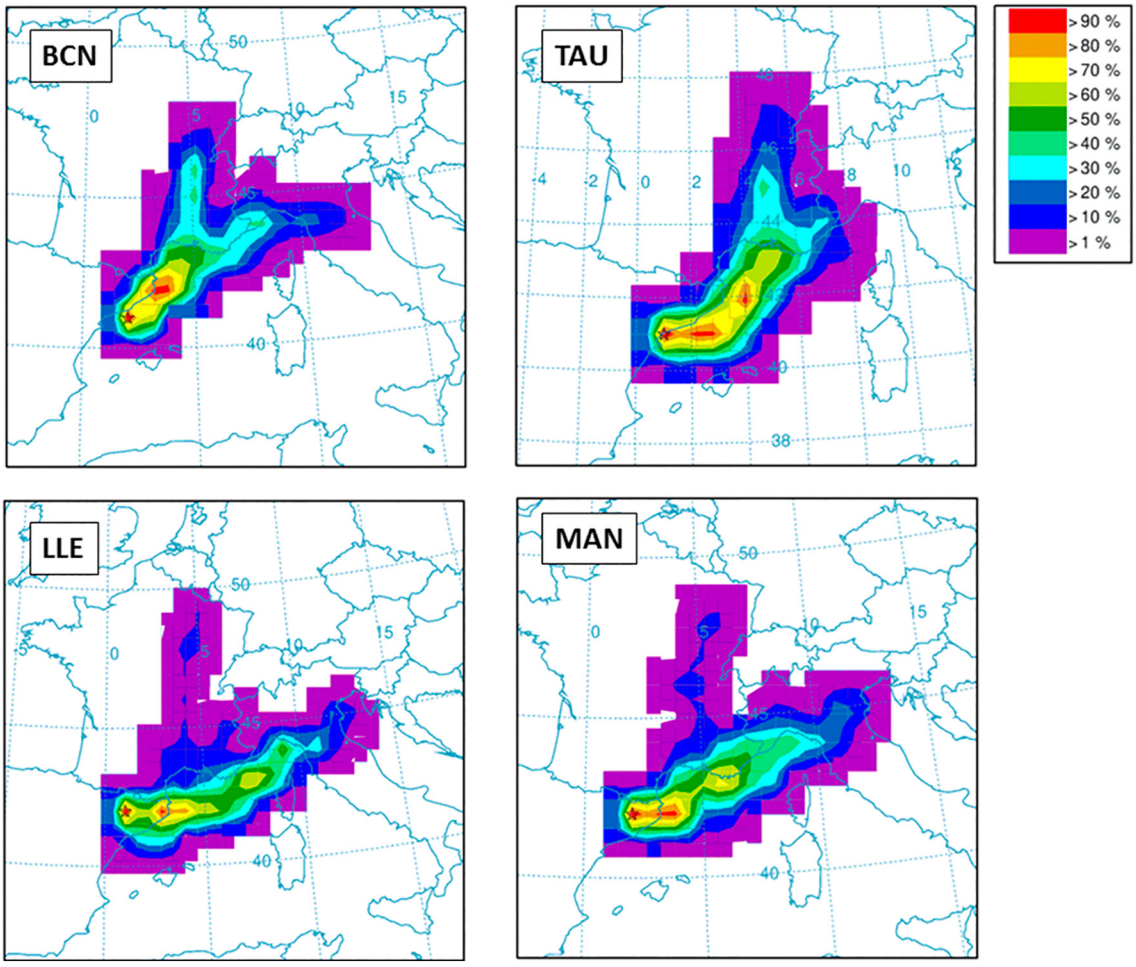

Fig. 7. HYSPLIT integrated back trajectories (number of trajectories passing through each 1° × 1° grid square, divided by the number of trajectories and expressed in percentages) for the PREVIOUS episode of 18 April 2007, ending at the stations BCN, TAU, LLE and MAN.

high-pressure system occurs over IP, resulting in a northwesterly flow over Catalonia, which sweeps across the entire Pyrenean region from west to east. This episode corresponded to a peak day that was simultaneous in all the stations, giving the highest values at GIC, BCN, and TAU. Aside from this Pyrenean influence, the HYSPLIT integrated back trajectories for the four represented stations also show remarkable transport from the

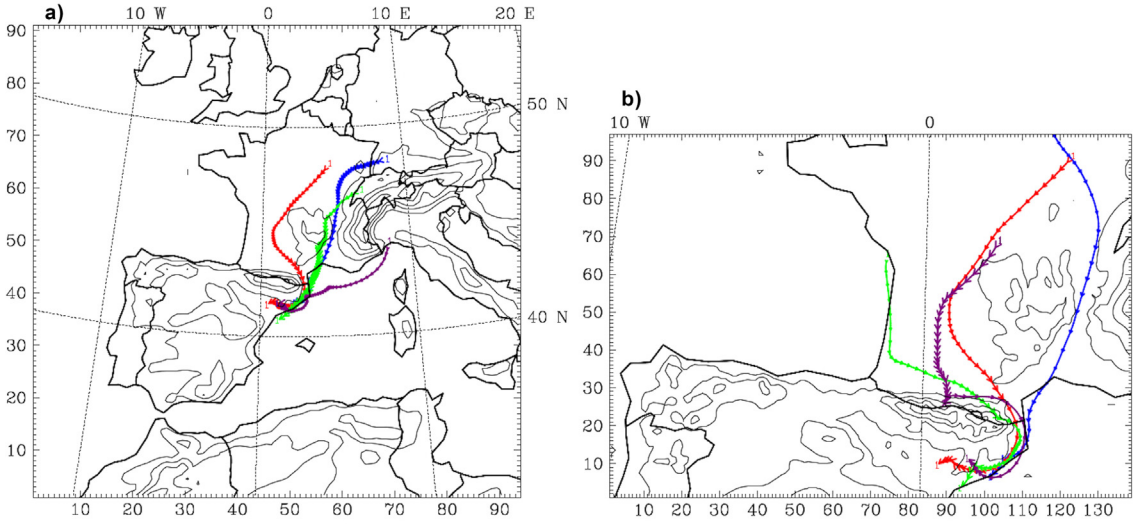

Fig. 8. WRF back trajectories computed in the domain a) D1 (27 km resolution) and b) D2 (9 km resolution) for the PREVIOUS episode of 18 April 2007, ending at the stations BCN (blue), TAU (green), LLE (red), and MAN (purple).

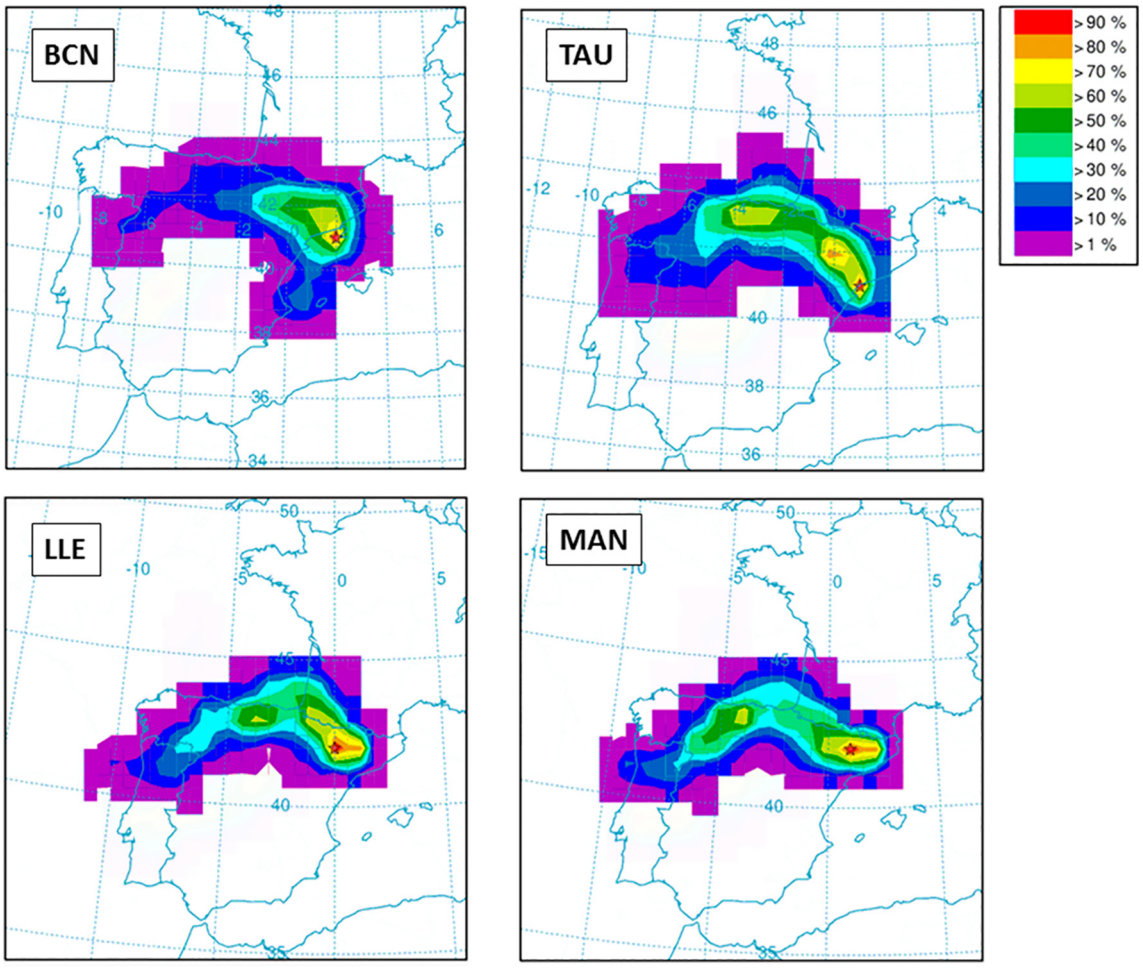

Fig. 9. Idem as Fig. 7 for the COINCIDENT episode of 27 April 2010.

Cantabrian forests of the Northern Iberian Peninsula and Galicia (north-western region) (Fig. 9). This flux probably affects the Catalan territory when it is channelled by the Ebro Valley.

This channelling is also discerned in the back trajectories obtained by WRF for D1 (Fig. 10), with the exception of MAN, which is more isolated from this influence, probably due to the barrier of the pre-coastal mountain range. This figure shows how the back trajectories of BCN and TAU come from the NW Iberian Peninsula. However, the back trajectories computed in D2 show that only LLE had Pyrenean transport, while that of BCN came from Central Europe, and those of TAU and MAN came from the

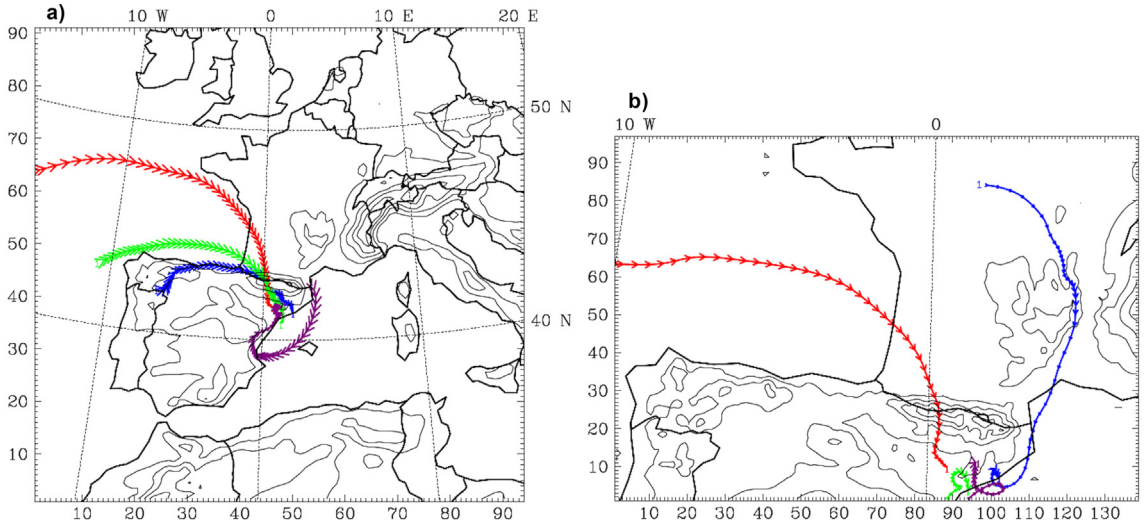

Fig. 10. Idem as Fig. 8 for the COINCIDENT episode of 27 April 2010.

south, although the latter two trajectories cannot be observed because they leave the domain.

3.4.3. LATER episode on the 18th of April 2014

The synoptic chart corresponding to the 18th of April 2014 shows the anticyclone to the west of the British Isles (see Fig. 6c) and the presence of a secondary high-pressure system over Central Europe. The flux is channelled between these two systems, entering Catalonia from the northwest. The most affected stations were GIC and MAN, much less so LLE, and TAU was not affected. The integrated back trajectories in Fig. 11 come from Central and Western France. The figure also shows that the southern station, TAU, had a lower percentage of back trajectories coming from France than did the other stations.

The WRF analysis (Fig. 12) shows a uniform flux crossing the Pyrenees from the Western France in D1. In the highest-resolution domain (D2) of the simulation, the back trajectories reaching TAU and LLE did not travel through the Pyrenees but instead penetrated from the Atlantic directly through the Ebro Valley. In the case of this later episode, the western character of the dominant flux indicates that the *Betula* origin was mainly Pyrenean.

4. Discussion

The 43 simultaneous peaks obtained in total over the 15-year period represent nearly three long-range transport episodes of *Betula* pollen per year over the Catalan territory, with pollen concentrations that affect the aerobiological stations differently, depending on their geographical location. The proportion of pollen contained in the peak dates was 38% of the *Betula* PPIn. Moreover, taking into account that these intrusions lasted longer than one day, the total pollen concentration per episode and the percentages involved were considerably higher. Estimates made considering also the pollen concentration for the days before and after each peak raised this percentage to near 60%.

The estimated quantities, shown in Table 5, reveal that, in the episodes produced on dates that do not coincide with the Pyrenees pollen season (i.e. PREVIOUS + LATER), the *Betula* pollen coming from the French Central Massif (FCM) and Central Europe (CEU) is nearly three times greater than that coming from the Pyrenees and the Northern Iberian Peninsula (2598 Pollen*day/m^3 vs. 1024 Pollen*day/m^3). However, for the episodes produced during the Pyrenees pollen season (COINCIDENT), the pollen concentration from the Pyrenees and the Northern Iberian Peninsula were considerably greater than those from France and Central Europe (769 Pollen*day/m^3 vs. 489 Pollen*day/m^3).

In the LATER cases, the back trajectories show a shorter residence time in PYR + NIP than in FCM + CEU (36% vs. 64%, Table 3). This means that the LATER episodes also resulted mainly from France and Central Europe transport, but with an important mix of pollen coming from the Pyrenees. The NIP residual contribution in the LATER episodes (4%) contrasts with the incidence of this region in the other clusters, especially in the COINCIDENT group, in which NIP (33%) surpassed the PYR contribution (28%).

In terms of measured totals, the station that received the highest percentage of *Betula* pollen (Table 2, sum of all episodes) is TAU (49%) and the lowest is GIC (30%). This can be explained by the geographical location of the sites. GIC is the northernmost station, close to the Pyrenees, and it is also the most influenced by local *Betula* pollen. This fact would explain the

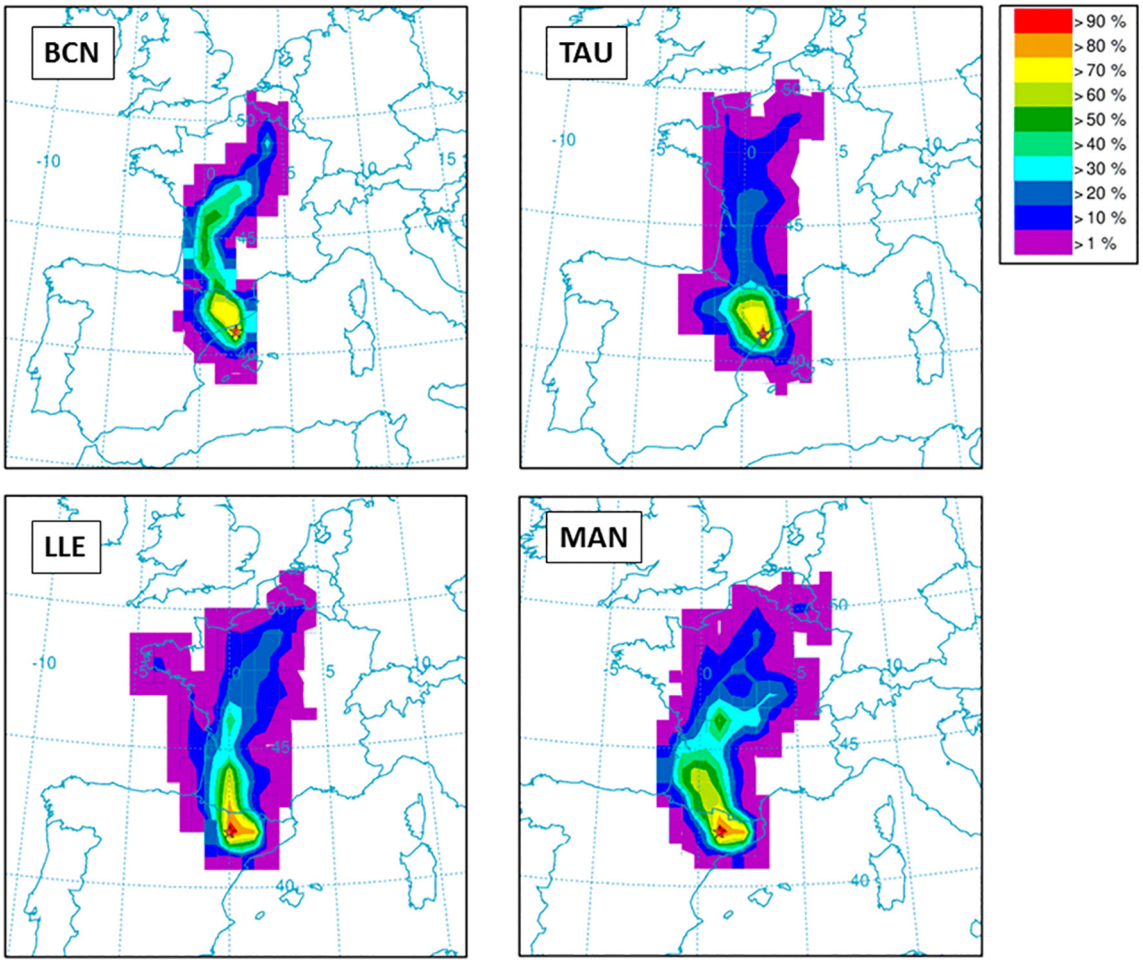

Fig. 11. Idem as Fig. 7 for the LATER episode of 18 April 2014.

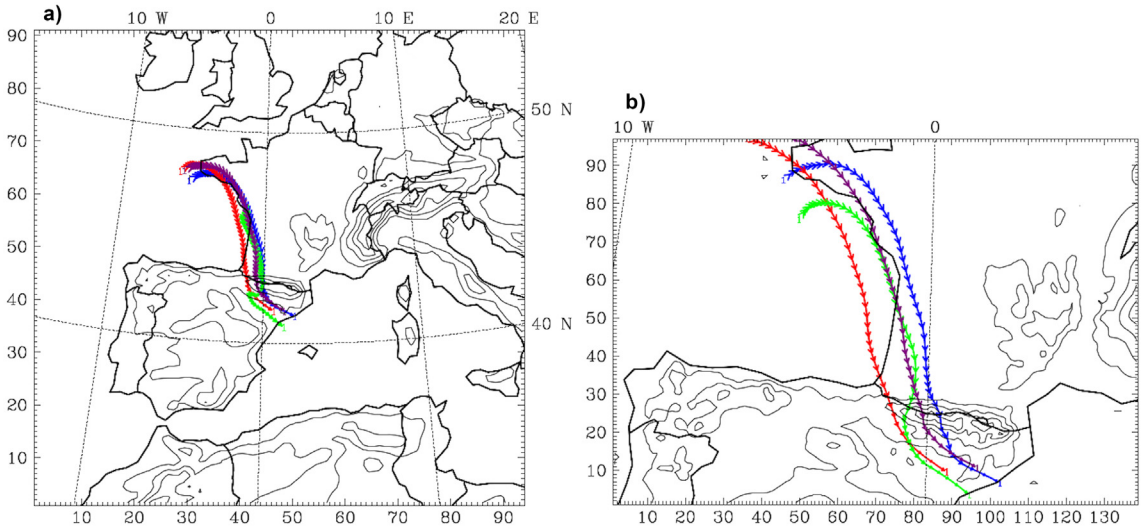

Fig. 12. Idem as Fig. 8 for the LATER episode of 18 April 2014.

high values of GIC in the different clusters (Table 2) in spite of the low percentage that represent. Conversely, TAU is the most southern station and the farthest from local sources. Furthermore, TAU is the station that received the highest contribution of PREVIOUS episodes (25% of its Pollen Integral, Table 2), which, as previously discussed, come mainly from European sources.

On the other hand, LLE and MAN show lower pollen concentration in the PREVIOUS episodes than the other stations, In fact, LLE is the station presenting the lowest values in the PREVIOUS cluster, with COINCIDENT being the cluster with the highest mean concentration by peak (12 Pollen/m^3 compared to 9 Pollen/m^3 for PREVIOUS and 5 Pollen/m^3 for LATER). These differences between inland and coastal stations can be explained by differences in the origins and paths of the air masses reaching the stations. Earlier studies (Belmonte et al., 2008; Izquierdo et al., 2017) stated that the Pyrenees acts as a barrier to the northerly fluxes, while the main path by which European air-masses enter the NE of Spain is the passage of Alberes at the easternmost end of the Pyrenees Massif, where the mountain ranges are considerably lower than in the central region. Fluxes that come from Europe and pass through this northeasterly passage impact the coastal and eastern sites (BCN, BTU, TAU, and GIC), and they partially affect the central sites (MAN) (Fig. 13). This would explain the high incidence of the PREVIOUS peaks in TAU, which is the most southern site. Conversely, this transport mechanism would have a minor impact on the western regions (LLE). Although all the episodes account for 32% (Table 2) of LLE's total pollen concentration (slightly higher than GIC), this station generally registered much lower pollen concentration than the other stations, which is somewhat surprising given that LLE receives the Pyrenees fluxes more directly. In contrast, the high residence time of the NIP trajectories obtained for LLE (Table 4) during COINCIDENT episodes reveals that the main transport entrance for the western and central Catalan regions is most likely through the Ebro Valley channel by means of the mesoscale northwest wind called Cierzo, which occurs frequently under synoptic situations of northerly advection (Fig. 13). Alternatively, the Cierzo wind could also contribute to the high TAU values during the PREVIOUS episodes mentioned above. The effect of this channelization has also been recently described in the study of an episode of *Pinus* pollen in Catalonia (Sicard et al., 2021) characterized by a dispersion of pollen grains towards the Mediterranean Sea, mainly driven by the northwesterly winds, from regions with a high presence of this tree. The study concludes that regular outbreaks of plumes with high concentrations of pollen are transported hundreds of kilometres to the Mediterranean Sea through this valley.

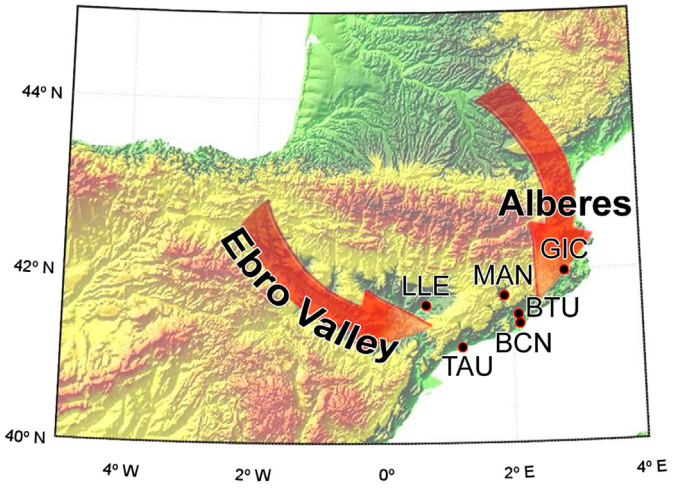

Fig. 13. Red arrows indicate the two main transport routes for *Betula* pollen entering the NE Iberian Peninsula: Alberes passage and Ebro Valley.

The present work has focused on studying simultaneous episodes in which the synoptic scale has been found to be mainly responsible for pollen transport. Using a high-resolution mesoscale model provided complementary information that has helped us interpret the measurements. The WRF analysis of the event occurred on 18th of April 2007 supports that the PREVIOUS episodes correspond to air mass inflows from Europe (FCM and CEU) through the Alberes pass. Figs. 7 and SM3 show back trajectories following this pattern in both domains and for all stations.

One of the most important mesoscale effects in the NE Iberian Peninsula is that of the sea breeze, which plays an important role in pollution episodes over coastal regions. In the Spanish Mediterranean coast these effects have been described linked to the formation of the Iberian thermal low (Millán et al., 1991), mainly in summer days, and related with intensive ozone episodes (Querol et al., 2016). The effect of mesoscale fluxes on regional and LRT of Poaceae pollen was described by Gassmann et al. (2002) finding an increase in pollen concentration after the occurrence of the breeze due to the re-entry of pollen caused by air recirculation. Negral et al. (2021) observed a reduction in the *Olea* pollen concentrations during marine advections in a coastal Mediterranean Spanish site due to the inhibition of the continental transport. Regarding Catalonia, the breeze effect is highly relevant because, in addition to the Ebro river, various other rivers that collect the rain water from the pre-coastal and pre-Pyrenean mountain ranges flow to the Catalan coast. This mesoscale circulation, which usually

predominates in spring and summer over the dominant synoptic situation, enters through the valleys of these rivers hundreds of kilometres inland. The most important river is the Llobregat, located in the centre of Catalonia, and it flows into the sea near Barcelona. The WRF simulation obtained for the COINCIDENT case study suggests that the northerly flow is inhibited in the central and inner regions by the sea breeze, which is channelled by the Llobregat river, as revealed by the back-trajectories of MAN in D1. The effect of the breeze is also evident in MAN and TAU for this episode in D2. On the other hand, the high-resolution trajectories of the LATER case study explain the low levels measured in LLE and TAU during the episode, since they show a direct entry from the Cantabrian Sea to the Ebro Valley through the western end of the Pyrenees.

Therefore, the present analysis states that air-masses highly loaded with *Betula* pollen take different paths to enter the NE Iberian Peninsula. During early spring, mainly the two middle weeks of April when pollination has not yet occurred in the Pyrenees, an important ingress of *Betula* pollen arrives from the FCM, which has already begun to release its pollen due to the lower altitude. This transport is produced by fluxes entering Catalonia mostly through the Alberes passage in few but highly loaded episodes, and it affects not only the northeastern sites of Barcelona (BCN), Bellaterra (BTU) and Girona (GIC), but also the southern coastal site of Tarragona (TAU), which would explain the high values registered at this site during the episodes of 18th and 19th of April 2007. It is likely that part of this northerly flux passes over the Pyrenees to also produce simultaneous pollen peaks at the central stations.

The pollen season in the birch forest of CEU is produced later, during the last week of April and the first half of May, due to its higher altitude and latitude. The transport from this region covers larger distances than that of FCM, and the loads reaching Catalonia are lower. It is probable that these air-masses arriving in the northeast of Spain mix with pollen from the French Central Massif and the Northern Iberian Peninsula. Transport from CEU affects all the stations, but the western regions to a lesser extent, as indicated by the low CEU residence time values obtained in Lleida (LLE) (Table 3).

The other important source of *Betula* pollen in Catalonia is the pollination in the Pyrenees, which is produced mainly in the short period between 24th and 29th of April. The input mechanism is transport by either air-masses originating in the Pyrenees region or by the passage of northerly fluxes over the Pyrenees. The whole Catalan territory is under its influence, but the northern regions are the most affected due to their proximity. Table 5 suggests that transport from the Northern Iberian Peninsula is also prominent during this period. Therefore, regarding the episodes that are COINCIDENT with the Pyrenees pollen season, the other contribution is the pollen coming from the Northern Iberian Peninsula, which enters Catalonia mostly through the Ebro Valley and reaches the southern regions. The high residence time in NIP for the TAU trajectories (Table 3) supports this interpretation. In addition, the pollen emission in PYR and NIP occurs on intermediate dates between the FCM and CEU emissions, and it is likely that a significant fraction of the air masses reaching Catalonia during these dates came from FCM and they transported a considerable amount of pollen from this region.

We have shown that long range *Betula* pollen transport over Catalonia has a great temporal variability, covering from early April to middle May, probably due to the considerable difference in latitude and height of the potential source areas. This contrast with the distant transport described by Bogawski et al. (2019b) over Poland, which mainly occurs in the first fortnight of May, and it is originated at higher latitude, mostly in Northwestern Russia where flowering usually starts later. However the meteorological mechanism responsible is similar in Catalonia and Poland: a high pressure system situated at high latitude, in Western Europe in the case of Catalonia, and displaced over Scandinavia and Northern Russia in the case of Poland. On the other hand, the differences we find in intensity and frequency between the three clusters could be partially explained by the different proximity of the source regions. In the case of the LATER episodes, presenting the lowest concentrations, it is very probably that a part of the pollen come from very distant sources as Scandinavia and Russia as indicated by the analysis of Bogawski et al. (2019b) confirming the findings of Siljamo et al. (2008) that, in some transport episodes, the whole of Europe can be in the range of a birch pollen cloud transported from Russia.

An interesting aspect to be studied in the future, which is outside the scope of this work, is the different allergenic load of pollen depending on the latitude and altitude of the monitoring site. An interesting work of Jochner et al. (2015) in the Alps at two different altitudes (734 and 2650 m a.s.l.) obtained that the calculated seasonal mean allergen release per pollen grain was higher in the valley than in the high altitude site. Given the diversity of *Betula* distant sources in Catalonia and the complexity of the Catalan territory, further research should be addressed to this issue when evaluating the clinical impact of the pollen intrusions.

5. Conclusions

This is the first study to quantify the contributions of the different distant source regions to the *Betula* pollen registered in Catalonia. Nearly 40% of the monitored pollen corresponded to long-range transport, which occurred every year in several episodes. Based on the residence time of the air-masses, we estimate that 37% of this *Betula* pollen came from the Pyrenees and Northern Iberian Peninsula, while 63% came from the French Central Massif (44%) and Black Forest / Vosges Massif (19%).

Back-trajectories show that most of the peak days corresponded to situations of northerly advection favoured by the presence of a high pressure centre over Northwestern Europe. In a certain way, the Pyrenees act as a barrier, which the air masses bypass as they are channelled through two entry routes to Catalonia (Fig. 13). One of these is the Alberes passage at the eastern end of the Pyrenees, and the other is the Ebro Valley, with the characteristic northwest wind of this region called the Cierzo.

Our analysis highlights the following points:

- The average pollen concentration contributed by each isolated peak in the episodes previous to the pollination in the Pyrenees was greater than those during the pollen season in the Pyrenees and was almost triple that of those after pollination in the Pyrenees.
- In early spring, prior to the pollen season in the Pyrenees, fast and highly loaded air masses arriving from the French Central Massif and Black Forest/Vosges Massif are responsible for important *Betula* pollen concentrations entering through the Alberes passage. This flux first impacts the most northern and eastern sites. On the other hand, the Ebro Valley also channels part of this flux and affects the western and southern regions.
- During the pollen season in the Pyrenees, slower air masses arriving from the Pyrenean forests affect the entire Catalan territory, but especially the central regions. At the same time, pollination occurs in the Northern Iberian Peninsula. The transport of this pollen from Galicia and the Cantabrian Mountain range significantly affects areas influenced by the Cierzo wind: the west, the south, and, to a lesser extent, the central areas of Catalonia.
- The episodes that occurred after the Pyrenean pollen season also provided significant levels of *Betula* pollen in the Northeast Iberian Peninsula. In these episodes, a mixture of pollen from different sources probably constitutes a greater proportion than in the others. However, while the main sources in these episodes are the Pyrenees and French Central Massif, Central Europe is also appreciable, while the Cantabrian Mountain range contribution is nearly null.
- The trajectories obtained with the WRF mesoscale model for three analyzed episodes have been consistent with what was stated above, and they have helped in its interpretation. In addition, they have highlighted the important role of mesoscale circulations over the Catalan territory. This is particularly important for the sea breeze as it channels inland through the course of the main rivers , inhibiting the transport of *Betula* during the northern advection situations, that moslty affects the central regions of Catalonia.

Supplementary data to this article can be found online at https://doi.org/10.1016/j.scitotenv.2021.151827.

CRediT authorship contribution statement

Marta Alarcón: methodology, writing, original draft preparation, HYSPLIT model, meteorology.
Cristina Periago:: meteorology, writing- Reviewing.
David Pino: WRF model, writing- reviewing.
Jordi Mazón: WRF model, writing- reviewing.
Maria del Carme Casas-Castillo: figures, writing- reviewing.
Jiang Ji Ho-Zhang: figures, writing- reviewing.
Concepción De Linares: pollen data, aerobiology, writing- reviewing.
Raül Rodríguez-Solà: figures, writing- reviewing.
Jordina Belmonte: pollen data, aerobiology, writing- reviewing.

Declaration of competing interest

The authors declare that they have no known competing financial interests or personal relationships that could have appeared to influence the work reported in this paper.

Acknowledgements

We acknowledge the financial support of the European Commission for ENV4-CT98-0755; the Spanish Government for CGL2004-21166-E, CGL2005-07543/CLI, CGL2009-11205, CGL2012-39523-C02-01/CLI, CGL2012-39523-C02-02, CGL2016-75996-R, CTM2017-89565-C2-1, CTM2017-89565-C2-2, and CSD 2007-00067; the Catalan Government for 2005SGR00519, 2009SGR1102, and 2017SGR1692; Diputació de Tarragona; Servei Meteorològic de Catalunya; Sociedad Española de Alergología e Inmunología Clínica (SEAIC); Laboratorios LETI PHARMA; Societat Catalana d'Al·lèrgia i Immunologia Clínica (SCAIC); J Uriach y Compañia; S.A. This research contributes to the "María de Maeztu" Programme for Units of Excellence of the Spanish Ministry of Science and Innovation (CEX2019-000940-M). The authors gratefully acknowledge the NOAA Air Resources Laboratory (ARL) for their HYSPLIT transport and dispersion model and the synoptic charts used in this publication.

References

Aira, M.J., Ferreiro, M., Iglesias, I., Jato, V., Marcos, C., Varela, S., Vidal, C., 2001. Aeropalinologia de cuatro ciudades de Galicia y su incidencia sobre la sintomatología alérgica estacional. In: Renduelles, B., Moreno, J. (Eds.), Moreno E. Proceedings of the XIII Simposio de la A.P.L.E. University of Cartagena, Cartagena, Spain, pp. 105–114.

Artz, R., Pielke, R.A., Galloway, J., 1985. Comparison of the ARL/ATAD constant level and the NCAR isentropic trajectory analyses for selected case studies. Atmos. Environ. 19, 47–63.

Beck, P., Caudullo, G., de Rigo, D., Tinner, W., 2016. Betula pendula, Betula pubescens and other birches in Europe: distribution, habitat, usage and threats. In: San-Miguel-Ayanz, J., de Rigo, D., Caudullo, G., Houston Durrant, T., Mauri, A. (Eds.), European Atlas of Forest Tree Species. Publ. Off. EU, Luxembourg, p. e010226 https://doi.org/10.2788/4251 ISBN 978-92-79-36740-3.

Begum, B.A., Kim, E., Jeong, C., Lee, D., Hopke, P.K., 2005. Evaluation of the potential source contribution function using the 2002 Quebec forest fire episode. Atmos. Environ. 39, 3719–3724.

Belmonte, J., Vendrell, M., Roure, J.M., Vidal, J., Botey, J., Cadahía, A., 2000. Levels of Ambrosia pollen in the atmospheric spectra of Catalan aerobiological stations. Aerobiologia 16, 93–99.

Belmonte, J., Alarcón, M., Àvila, A., Scialabba, E., Pino, D., 2008. Long-range transport of beech (Fagus sylvatica L.) pollen to Catalonia (north-eastern Spain). Int. J. Biometeorol. 52, 675–687.

Bogawski, P., Borycka, K.P., Grewling, L., Kasprzyk, I., 2019a. Detecting distant sources of airborne pollen for Poland: integrating back-trajectory and dispersion modelling with a satellite-based phenology. Sci. Total Environ. 689, 109–125. https://doi.org/10.1016/j.scitotenv.2019.06.348.

Bogawski, P., Grewling, L., Jackowiak, B., 2019b. Predicting the onset of Betula pendula flowering in Poznań (Poland) using remote sensing thermal data. Sci. Total Environ. 658, 1485–1499. https://doi.org/10.1016/j.scitotenv.2018.12.295.

Chen, F., Dudhia, J., 2001. Coupling an advanced land surface–hydrology model with the Penn State–NCAR MM5 modeling system. Part I: model implementation and sensitivity. Mon. Weather Rev. 129, 569–585.

D'Amato, G., Cecchi, L., Bonini, S., Nunes, C., Annesi-Maesano, I., Behrendt, H., Liccardi, G., Popov, T., van Cauwenbergh, P., 2007. Allergenic pollen and pollen allergy in Europe. Allergy 62, 976–990.

Damialis, A., Gilles, S., Sofiev, M., Sofieva, V., Kolek, F., Bayr, D., Plaza, M.P., Leier-Wirtz, V., Kaschuba, S., Ziska, L.H., Bielory, L., Makra, L., Trigo, M.M., COVID-19/POLLEN study group, Traidl-Hoffmann, C., 2021. Higher airborne pollen concentrations correlated with increased SARS-CoV-2 infection rates, as evidenced from 31 countries across the globe. Proc. Natl. Acad. Sci. 118 (12), e2019034118. https://doi.org/10.1073/pnas.2019034118 Mar 2021.

Dayan, U., Lamb, D., 2003. Meteorological indicators of summer precipitation chemistry in central Pennsylvania. Atmos. Environ. 37, 1045–1055.

De Bolòs, O., Vigo, J., Masalles, R.M., Ninot, J.M., 1990. Flora manual dels països Catalans. Editorial Pòrtic SA, pp. 1–1310.

De Weger, L.A., Bergmann, K.C., Rantio-Lehtimäki, A., Dahl, A., Buters, J., Déchamp, Ch., Belmonte, J., Thibaudon, M., Cecchi, L., Besancenot, J.-P., Galán, C., Waisel, Y., 2013. Impact of pollen. In: Sofiev, M., Bergmann, K.-C. (Eds.), Allergenic Pollen: A Review of the Production, Release, Distribution and Health Impacts https://doi.org/10.1007/978-94-007-4881-1_6.

Dopazo, A., 2001. Variación estacional y modelos predictivos de polen y esporas aeroalergénicos en Santiago de Compostela. Universidad de Santiago de Compostela Tesis Doctoral.

Draxler, R.R., Rolph, G.D., 2003. HYSPLIT (HYbrid Single-particle Lagrangian Integrated Trajectory) Model Access Via NOAA ARL READY Website. NOAA Air Resources Laboratory, Silver Spring, MD. http://www.arl.noaa.gov/ready/HYSPLIT4.html.

Dudhia, J., 1989. Numerical study of convection observed during the winter monsoon experiment using a mesoscale two–dimensional model. J. Atmos. Sci. 46, 3077–3107.

Emberlin, J., Savage, M., Jones, M., 1993. Annual variations in grass pollen seasons in London 1961–1990: trends and forecast models. Clin. Exp. Allergy 23 (11), 911–918.

Emberlin, J., Mullins, J., Corden, J., Millington, W., Brooke, M., Savage, M., Jones, S., 1997. The trend to earlier birch pollen seasons in the U.K.: a biotic response to changes in weather conditions? Grana 36 (1), 29–33.

Erdtman, O.G., 1992. In: Nilsson, S., Praglowski, J. (Eds.), Handbook of Palynology, 2nd edition. Munksgaard, Copenhagen (580 pp.).

Fernández-Llamazares, A., Belmonte, J., Alarcón, M., López-Pacheco, M., 2012. Ambrosia L. in Catalonia (NE Spain): expansion and aerobiology of a new bioinvader. Aerobiologia https://doi.org/10.1007/s10453-012-9247-1.

Fernández-Llamazares, A., Belmonte, J., Delgado, R., De Linares, C., 2014. A statistical approach to bioclimatic trend detection in the airborne pollen records of Catalonia (NE Spain). Int. J. Biometeorol. 58, 371–382.

Galán, C., Cariñanos, P., Alcázar, P., Domínguez-Vilches, E., 2007. Manual de Calidad y Gestión de la Red Española de Aerobiología. Servicio de Publicaciones, Universidad de Córdoba.

Galán, C., Smith, M., Thibaudon, M., Frenguelli, G., Oteros, J., Gehrig, R., EAS QC working group, 2014. Pollen monitoring: minimum requirements and reproducibility of analysis. Aerobiologia 30 (4), 385–395.

García-Mozo, H., Hernández-Ceballos, M.A., Trigo, M.M., Galán, C., 2017. Wind dynamics' influence on south Spain airborne olive-pollen during african intrusions. Sci. Total Environ. 609, 1340–1348.

Gassmann, M.I., Pérez, C.F., Gardiol, J.M., 2002. Sea–land breeze in a coastal city and its effect on pollen transport. Int. J. Biometeorol. 46, 118–125. https://doi.org/10.1007/s00484-002-0135-1.

Grewling, Ł., Bogawski, P., Jenerowicz, D., Czarnecka-Operacz, M., Sikoparija, B., Skjøth, C.A., Smith, M., 2016. Mesoscale atmospheric transport of ragweed pollen allergens from infected to uninfected areas. Int. J. Biometeorol. 60 (10), 1493–1500.

Grinn-Gofroń, A., Çeterb, T., Pinarc, N.M., Bosiackad, B., Çeterc, S., Keçelie, T., Myśliwyd, M., Şahinc, A.A., Bogawskif, P., 2020. Airborne fungal spore load and season timing in the Central and Eastern Black Sea region of Turkey explained by climate conditions and land use. Agric. For. Meteorol. 296, 1081–1091.

Grinn-Gofroń, A., Bogawski, P., Bosiacka, B., Nowosad, J., Camacho, I., Sadyś, M., Skjøth, C.A., Pashley, C.H., Rodinkova, V., Çeter, T., Traidl-Hoffmann, C., Damialis, A., 2021. Abundance of Ganoderma sp. in Europe and SW Asia: modelling the pathogen infection levels in local trees using the proxy of airborne fungal spore concentrations. Sci. Total Environ. 793, 148509. https://doi.org/10.1016/j.scitotenv.2021.148509 Epub 2021 Jun 18. PMID: 34175598.

Heinzerling, L.M., Burbach, G.J., Edenharter, G., Bachert, C., Bindslev-Jensen, C., Bonini, S., Bousquet, J., Bousquet-Rouanet, L., Bousquet, P.J., Bresciani, M., et al., 2009. GA2LEN skin test study I: GA2LEN harmonization of skin prick testing: novel sensitization patterns for inhalant allergens in Europe. Allergy 64, 1498–1506.

Hernández-Ceballos, M.A., García-Mozo, H., Adame, J.A., Domínguez-Vilches, J.A., Bolívar, J.P., De la Morena, B.A., Pérez-Badía, R., Galán, C., 2011. Determination of potential sources of Quercus airborne pollen in Córdoba city (southern Spain) using back-trajectory analysis. Aerobiologia 27 (3), 261–276. https://doi.org/10.1007/s10453-011-9195-1.

Hernández-Ceballos, M.A., Skjøth, C.A., García-Mozo, H., Bolívar, J.P., Galán, C., 2014. Improvement in the accuracy of back trajectories using WRF to identify pollen sources in southern Iberian Peninsula. Int. J. Biometeorol. 58 (10), 2031–2043. https://doi.org/10.1007/s00484-014-0804-x.

Hernández-Ceballos, M.A., García-Mozo, Galán, C., 2015. Cluster analysis of intradiurnal holm oak pollen cycles at peri-urban and rural sampling sites in southwestern Spain. Int. J. Biometeorol. 59 (8), 971–982. https://doi.org/10.1007/s00484-014-0910-9.

Hirst, J., 1952. An automatic volumetric spore trap. Ann. Appl. Biol. 39 (2), 257–265.

Hong, S.H., Pan, H.L., 1996. Nonlocal boundary layer vertical diffusion in a medium–range forecast model. Mon. Weather Rev. 124, 2322–2339.

Hong, S.Y., Dudhia, J., Chen, S.H., 2004. A revised approach to ice microphysical processes for the bulk parameterization of clouds and precipitation. Mon. Weather Rev. 132, 103–120.

Izquierdo, R., Belmonte, J., Àvila, A., Alarcón, M., Cuevas, E., Alonso-Pérez, S., 2011. Source areas and long-range transport of pollen from continental land to Tenerife (Canary Islands). Int. J. Biometeorol. 55, 67–85.

Izquierdo, R., Alarcón, M., Majeed, H.T., Periago, C., Belmonte, J., 2015a. Influence of atmospheric teleconnection patterns on airborne pollen levels in the NE Iberian Peninsula. Clim. Res. 66 (2), 171–183.

Izquierdo, R., Alarcon, M., Periago, C., Belmonte, J., 2015b. Is long-range transport of pollen in the NW Mediterranean basin influenced by Northern Hemisphere teleconnection patterns? Sci. Total Environ. 532, 771–779.

Izquierdo, R., Alarcón, M., Mazón, J., Pino, D., De Linares, C., Aquinagalde, X., Belmonte, J., 2017. Are the Pyrenees a barrier for the transport of birch (Betula) pollen from Central Europe to the Iberian Peninsula? Sci. Total Environ. 575 (2017), 1183–1196.

Jochner, S., Luepke, M., Laube, J., Weichenmeier, I., Pusch, G., Traidl-Hoffmann, C., Schmidt-Weber, C., Buters, J.T.M., Menzel, A., 2015. Seasonal variation of birch and grass pollen loads and allergen release at two sites in the German Alps. Atmos. Environ. 122, 83–93. https://doi.org/10.1016/j.atmosenv.2015.08.031.

Mahura, A.G., Korsholm, U.S., Baklanov, A.A., Rasmusen, A., 2007. Elevated birch pollen episodes in Denmark: contributions from remote sources. Aerobiologia 23, 171–179. https://doi.org/10.1007/s10453-007-9061-3.

Millán, M.M., Artíñano, B., Alonso, L.A., Navazo, M., Castro, M., 1991. The effect of mesoscale flows on regional and long-range atmospheric transport in the western Mediterranean area. Atmos. Environ. 25, 949–963.

Mlawer, E.J., Tubman, S.J., Brown, P.D., Iacono, M.J., Clough, S.A., 1997. Radiative transfer for inhomogeneous atmospheres: RTM, a validated correlated–k model for the long wave. J. Geophys. Res. 102, 663–682.

Myszkowska, D., Majewska, R., 2014. Pollen grains as allergenic environmental factors–new approach to the forecasting of the pollen concentration during the season. Ann. Agric. Environ. Med. 21 (4), 681–688.

Myszkowska, D., Piotrowicz, K., 2009. Birch (Betula L.) pollen seasons in Cracow in 1991–2008 associated to the meteorological conditions. Acta Agrobot. 62 (2), 67–75.

Negral, L., Moreno-Grau, S., Galera, M.D., Elvira-Rendueles, B., Costa-Gómez, I., Aznar, F., Pérez-Badia, R., Moreno, J.M., 2021. The effects of continentality, marine nature and the recirculation of air masses on pollen concentration: olea in a Mediterranean coastal enclave. Sci. Total Environ. 790, 47999. https://doi.org/10.1016/j.scitotenv.2021.147999.

Ojrzyńska, H., Bilińska, D., Werner, M., Kryza, M., Malkiewicz, M., 2020. The influence of atmospheric circulation conditions on Betula and Alnus pollen concentrations in Wrocław, Poland. Aerobiologia 36, 261–276. https://doi.org/10.1007/s10453-020-09629-9.

Pereira, C., Valero, A., Loureiro, C., Dávila, I., Martinez-Cócera, C., Murio, C., Rico, P., Palomino, R., 2006. Iberian study of aeroallergens sensitisation in allergic rhinitis. Eur. Ann. Allergy Clin. Immunol. 38, 186–194.

Pfaar, O., Bastl, K., Berger, U., Buters, J., Calderon, M.A., Clot, B., Darsow, Demoly, U.P., Durham, S.R., Galán, C., Gehrig, R., Gerth van Wijk, R., Jacobsen, L., Klimek, L., Sofiev, Thibaudon, M.M., Bergmann, K.C., 2017. Defining pollen exposure times for clinical trials of allergen immunotherapy for pollen-induced rhinoconjunctivitis – an EAACI position paper. Allergy 72 (5), 713–722. https://doi.org/10.1111/all.13092.

Qin, X., Li, Y., Sun, X., Meng, L., Wang, X., 2019. Transport pathway and source area for Artemisia pollen in Beijing,China. Int. J. Biometeorol. 63, 687–699. https://doi.org/10.1007/s00484-017-1467-1.

Querol, X., Alastuey, A., Reche, C., Orio, A., 2016. On the origin of the highest ozone episodes in Spain. Sci. Total Environ. 572, 379–389. https://doi.org/10.1016/j.scitotenv.2016.07.193.

Robichaud, A., Comtois, P., 2017. Statistical modeling, forecasting and time series analysis of birch phenology in Montreal Canada. Aerobiologia 33 (4), 529–554. https://doi.org/10.1007/s10453-017-9488-0.

Sicard, M., Izquierdo, R., Alarcón, M., Belmonte, J., Comerón, A., Baldasano, J.M., 2016a. Near-surface and columnar measurements with a micro pulse lidar of atmospheric pollen in Barcelona, Spain. Atmos. Chem. Phys. 16 (11), 6805–6821. https://doi.org/10.5194/acp-16-6805-2016.

Sicard, M., Izquierdo, R., Jorba, O., Alarcón, M., Belmonte, J., Comerón, A., Baldasano, J.M., 2016b. Atmospheric dispersion of airborne pollen evidenced by near-surface and columnar measurements in Barcelona, Spain. In: Comerón, A., Kassianov, E.I., Schäfer, K., Jack, J.W., Picard, R.H., Weber, K. (Eds.), Proc. SPIE 10001, 100010L. SPIE, Washington (EE. UU.) https://doi.org/10.1117/12.2244517 Edinburgh, United Kingdom.

Sicard, M., Izquierdo, R., Jorba, O., Alarcón, M., Belmonte, J., Comerón, A., De Linares, C., Baldasano, J.M., 2017. Modelling of pollen dispersion in the atmosphere: evaluation with a continuous 1β+1δ lidar. Proc. of the 28th International Laser Radar Conference (ILRC28), EPJ Web of Conferences. 176. https://doi.org/10.1051/epjconf/201817605006 Bucharest (Romania).

Sicard, M., Jorba, O., Izquierdo, R., Alarcón, M., De Linares, C., Belmonte, J., 2019. Modelling of airborne pollen dispersion in the atmosphere in the Catalonia region, Spain: model description, emission scheme and evaluation of model performance for the case of Pinus. Proc.SPIE 11152, Remote Sensing of Clouds and the Atmosphere XXIV https://doi.org/10.1117/12.2534819.

Sicard, M., Jorba, O., Ho, J.J., Izquierdo, R., De Linares, C., Alarcón, M., Comerón, A., Belmonte, J., 2021. Measurement report: characterization of the vertical distribution of airborne Pinus pollen in the atmosphere with lidar-derived profiles: a modelling case study in the region of Barcelona,NE Spain. Atmos. Chem. Phys. https://doi.org/10.5194/acp-2021-235 (in press).

Siljamo, P., Sofiev, M., Severova, E., Ranta, H., Kukkonen, J., Polevova, S., Kubin, E., Minin, A., 2008. Sources, impact and exchange of early-spring birch pollen in the Moscow region and Finland. Aerobiologia 24, 211–230.

Skamarock, W.C., Klemp, J.B., Dudhia, J., Gill, D.O., Barker, D.M., Duda, M., Huang, X.Y., Powers, J.G., 2008. A Description of the Advanced Research WRF Version 3; Technical Report TN–475+STR. NCAR, Boulder, CO, USA.

Skjøth, C.A., Sommer, J., Stach, A., Smith, M., Brandt, J., 2007. The long-range transport of birch (Betula) pollen from Poland and Germany causes significant pre-season concentrations in Denmark. Clin. Exp. Allergy 37, 1204–1212. https://doi.org/10.1111/j.1365-2222.2007.02 771.x.

Skjøth, C.A., Smith, M., Brandt, J., Emberlin, J., 2009. Are the birch trees in southern England a source of Betula pollen for North London? Int. J. Biometeorol. 53 (1), 75–86.

Skjøth, C.A., Baker, P., Sadyś, M., Adams-Groom, B., 2015. Pollen from alder (Alnus sp.), birch (Betula sp.) and oak (Quercus sp.) in the UK originate from small woodlands. Urban Clim. 14, 414–428.

Sofiev, M., Siljamo, P., Ranta, H., Rantio-Lehtimaki, A., 2006a. Towards numerical forecasting of long-range air transport of birch pollen: theoretical considerations and a feasibility study. Int. J. Biometeorol. 50, 392–402.

Sofiev, M., Siljamo, P., Valkama, I., Ilvoven, M., Kukkonen, J., 2006b. A dispersión modelling system SILAM and its evaluation against ETEX data. Atmos. Environ. 40, 674–685.

Sofiev, M., Belmonte, J., Gebrig, R., Izquierdo, R., Smith, M., Dahl, A., Siljamo, P., 2006c. Airborne pollen transport. In: Sofiev, M., Bergmann, K.Ch. (Eds.), Allergenic Pollen. A Review of the Production, Release, Distribution and Health Impacts. Springer, Berlin, pp. 127–159.

Sofiev, M., Berger, U., Prank, M., Vira, J., Arteta, J., Belmonte, J., Bergmann, K.-C., Chéroux, F., Elbern, H., Friese, E., et al., 2015. MACC regional multi-model ensemble simulations of birch pollen dispersion in Europe. <sb:contribution></sb:contribution><sb:host><sb:issue><sb:series><sb:title>Atmos. Chem. Phys</sb:title></sb:series></sb:issue></sb:host> 15, 8115–8130.

Spieksma, F.T.M., Emberlin, J., Hjelmroos, M., Jäger, S., Leuschner, R.M., 1995. Atmospheric birch (Betula) pollen in Europe: trends and fluctuations in annual quantities and the starting date of the seasons. Grana 34, 51–57.

Stohl, A., 1996. Trajectory statistics-a new method to establish sourcereceptor relationships of air pollutants and its applications to the transport of particulate sulphate in Europe. Atmos. Environ. 30, 579–587.

Wotawa, G., Kröger, H., 1999. Testing the ability of trajectory statistics to reproduce emission inventories of air pollutants in cases of negligible measurement and transport errors. Atmos. Environ. 33, 3037–3043.